Electronic Supplementary Information (ESI):

In-situ Preparation of Nickel-oxy-hydroxide Decorated ITQ-2 Composite: A Hydrodeoxygenation Catalyst

*Naroth P. Nimisha, Soumya B. Narendranath, Ayyamperumal Sakthivel **

Inorganic Materials & Heterogeneous Catalysis Laboratory, Department of Chemistry,
School of Physical Sciences, Sabarmati Building, Tejawini Hills,
Central University of Kerala, Kasaragod - 671316, Kerala, India.
**Email: sakthiveldu@gmail.com / sakthivelcuk@cukerala.ac.in*
ORCID information: https://orcid.org/0000-0003-2330-5192

Experimental

Synthesis of MCM-22(P)

The MCM-22 with Si/Al = 30 and molar gel composition SiO_2:0.3 NaOH:0.033 Al_2O_3:0.5 HMI:45 H_2O was synthesised as per the modified procedure reported earlier.[1] A synthesis mixture containing aluminosilicate gel (colloidal silica; silicon (IV) oxide 50 wt.%, Alfa Aesar; sodium aluminate; $NaAlO_2$, Sigma Aldrich; (Al_2O_3): 50–56% and (Na_2O): 37–45%), NaOH (SRL, 98%), and the template HMI (98%; Alfa Aesar) was hydrothermally treated for 7 days at 155 °C. After the crystallisation period, the sample was washed with distilled water and ethanol and dried overnight at 70 °C to obtain the MCM-22 precursor, MCM-22 (P).

Preparation of Nickel-oxy-hydroxide Decorated ITQ-2 Composite

A slurry comprising 1 g of MCM-22 (P), an equimolar mixture of CTABr (25%, SRL) and CTAOH (TCI), 40 wt% TPAOH (Tritech), and 60 mL of water was refluxed at 70 °C for 24 hours with continuous stirring. After the treatment, the slurry was cooled to room temperature. The pH of the mixture was noted. The mixture was placed in an ultrasound bath (50 W, 40 kHz) for one hour to force the layers apart. The mixture was labelled MCM-22 (S). The nickel salt, viz., nickel nitrate hexahydrate ($Ni(NO_3)_2$. $6H_2O$, Loba Chemie), was added (5 –20 wt%) *in situ* to MCM-22 (S) with continuous stirring, followed by sonication and further refluxing at appropriate conditions. The mixture was then cooled to room temperature. The resultant pH was noted. The solid product was separated by centrifugation, subsequently dried in an air oven, and represented as Ni-ITQ-2 composite. The composition of the precursor mixture, nickel concentration, synthesis conditions by varying the metal concentration, and pH are listed in Table S1.

Table S1. Molar composition and synthesis condition of MCM-22(P) to Ni-ITQ-2 Composite.

MCM-22 (P) composition	1 SiO_2 : 0.0385 Al_2O_3 : 0.1468 NaOH : 0.353 HMI :0.04–0.07 $CTABr^-/OH^-$: 0.12 TPAOH : 30.5 H_2O.
Nickel concentration (range in mmol and mol %)	4.6-18 mol % (equivalent to 8.5-34.0 mmol with respect to silica)
pH (range)	2-13 (pH adjusted using con. HCl; (Fischer Scientific, 35.8 %)
Synthesis Conditions	70 °C, 48 h refluxing and 0.5 h sonication

For comparison, swollen MCM-22 (P) was delaminated by sonication in the absence of nickel oxy-hydroxide, with and without pH adjustment, and was labelled ITQ-2 and MS-1, respectively.

Similarly, pure nickel oxy-hydroxide was synthesised under the same conditions and represented as NiO(OH).

The post-synthetic nickel-loaded MCM-22 and ITQ-2 samples were prepared by using nickel nitrate hexahydrate ($Ni(NO_3)_2$. $6H_2O$) as the nickel source. In order to prepare 20 wt.% Ni-loaded samples, initially a $Ni(NO_3)_2.6H_2O$ solution is prepared by dissolving it in distilled water. The resultant $Ni(NO_3)_2$. $6H_2O$ solution was uniformly introduced into MCM-22 and ITQ-2 samples evenly spread on petri dishes by the incipient wetness method. Then the samples were kept overnight at room temperature for drying. Ni-loaded MCM-22 and ITQ-2 catalysts were calcined at 400 °C for 6 hours (2°/min), and the resultant samples were labelled Ni-MCM-22 and ITQ-2-Ni-W, respectively. The physical mixture was synthesised by simply grinding ITQ-2 and nickel oxy-hydroxide and labelled as ITQ-2-Ni-P.

Characterization

The powder XRD diffraction patterns were recorded using a D8 Advance (Brucker) X-ray diffractometer with Cu-Kα radiation (λ=1.54059 Å) in a 2θ range of 5–80°, a scan speed of 3° min^{-1}, and a step size of 0.02. FTIR spectra were recorded on a JASCO-FT/IR 4700 FTIR spectrophotometer. Spectra were collected with a resolution of 4 cm^{-1} and 60 scans in the mid-IR (400–4000 cm^{-1}) region. Brunauer-Emmett-Teller (BET) surface area and N_2 adsorption-desorption of the samples were determined at − 196 °C by an automatic micropore physisorption analyzer (Micromeritics ASAP 2020, USA) after the samples were degassed at 250 °C for 10 h. The BET surface area was calculated in the relative pressure range 0–0.1 over the adsorption branch of the isotherm. Barrette-Joyner-Halenda (BJH) pore size distribution was obtained from the desorption branch of the isotherm. Other textural properties, like pore volume, were elucidated from the isotherm data. The acid properties of H-type zeolites were obtained by temperature-programmed desorption of ammonia (NH_3-TPD) analysis using a BELCAT-M (Japan) TPD instrument equipped with a thermal conductivity detector (TCD). The sample was preheated in a quartz reactor at 400 °C for 30 minutes in a He flow. The ammonia was adsorbed at 50 °C for 30 min. Ammonia desorption was carried out at 50 °C for 15 minutes to remove any physisorbed ammonia. TPD of ammonia was performed from 50 to 900 °C at a heating rate of 10 °C/min in a hellium flow of 30 mL/min. A plot of the TCD signal versus temperature obtained was used to determine the number of acidic sites and their strength. The pyridine FT-IR spectrum was recorded using a Nicolet iS50 FTIR spectrometer (Thermo Fisher Scientific). The samples were pressed into a self-supporting wafer and pre-activated at 400 °C. The background spectrum was recorded

first after cooling the sample to room temperature. The pyridine was adsorbed on the samples at room temperature and allowed to saturate for 30 min. The pyridine desorption was performed from 50 to 350 °C. The FTIR spectrum was recorded and analysed for Brönsted and Lewis acidic sites. The morphologies of the samples were examined by a VEGA3 TESCAN-scanning electron microscope. High-resolution transmission electron microscopy (HRTEM) micrographs were obtained from an M/s JOEL JEM 2100 transmission electron microscope with a field emission gun operating at 200 kV. A custom-built ambient pressure photoelectron spectrometer (Prevac, Poland) that was equipped with a VG Scienta's R3000HP analyzer and a MX650 monochromator was utilised to obtain the X-ray photoelectron spectroscopy (XPS) data. The GC-MS of the product samples were recorded using Thermo Scientific Trace GC Ultra. ^{1}H NMR was performed using Bruker Ascend 500 at 500 MHz with $CDCl_3$ as solvent. The thermal stability of the fresh and used catalysts was assessed using a simultaneous thermal analyzer (STA 6000, PerkinElmer).

Catalytic Study

The HDO reaction was carried out in a 50-mL Teflon-lined autoclave. Prior to the reaction, the Ni-ITQ-2 composite catalysts were reduced under H_2 pressure at 400 °C for 4 h. In a typical experiment, *m*-cresol (2 mmol), the catalyst (50 mg contain 8 mol. % of Ni with respect to substrate concentration), and the solvent (*n*-dodecane, 2 mL) were added to the autoclave. The reactor was purged with hydrogen (2 MPa) and sealed; subsequently, the autoclave was placed at 170 °C for 6 h. After the reaction was complete, the reactor was cooled, and the liquid products were collected and analysed using a gas chromatograph (Mayura Analytical 1100 series, FID detector, and HP88 column) using a specified program (70–240 °C, 10° min^{-1}). The products of the reactions were confirmed with authentic samples. The GC patterns of the reaction mixture (Fig. S12) and the product (Fig. S13) are shown. Further, the same was analysed using FT-IR spectroscopy. The reaction mixture containing *m*-cresol and *n*-dodecane exhibits peaks characteristic of aromatic compounds, viz., aromatic ring vibration (3040 cm^{-1}; γ_{C-H}) and the weak combination and overtone bands in the 1650–1600 cm^{-1} region. The disappearance of these bands in the product mixture supports the hydrogenation of the ring and the loss of aromatic character (Fig. S11), hence the formation of methyl cyclohexane. The samples were further confirmed by the GC-MS data obtained. The product mixture was separated from the solvent (*n*-dodecane) by the distillation method, and the product was confirmed by ^{1}H NMR.

Hot Filtration tests

The catalyst was studied for hot filtration tests to check the metal (Ni) leaching. Initially the reaction was carried out as mentioned before (*m*-cresol: 2 mmol, 0.05g catalyst, *n*-dodecane: 2 mL, 170 °C, 2MPa) for a duration of 1 h. The catalyst was separated after one hour by filtration. The filtrate was analysed with GC to obtain the yield. The reaction was continued further with the filtrate for 5 h under the same reaction conditions. The yield was calculated from the GC analysis. The results were compared and found that no metal leaching has occurred. This confirms that nickel species is confined on the surface of ITQ-2 sheets (Fig. S).

Catalyst reactivation

The catalyst is recovered by filtration after the reaction. It was washed with isopropyl alcohol to remove any impurities physisorbed on catalyst surface and further dried. The catalyst was calcined at 550 °C for 6 h in presence of air to remove any unreacted molecules or coke deposited on surface. The calcined catalyst was finally reduced in the presence of H_2 at 400 °C for 4 h, thus obtaining the recovered catalyst.

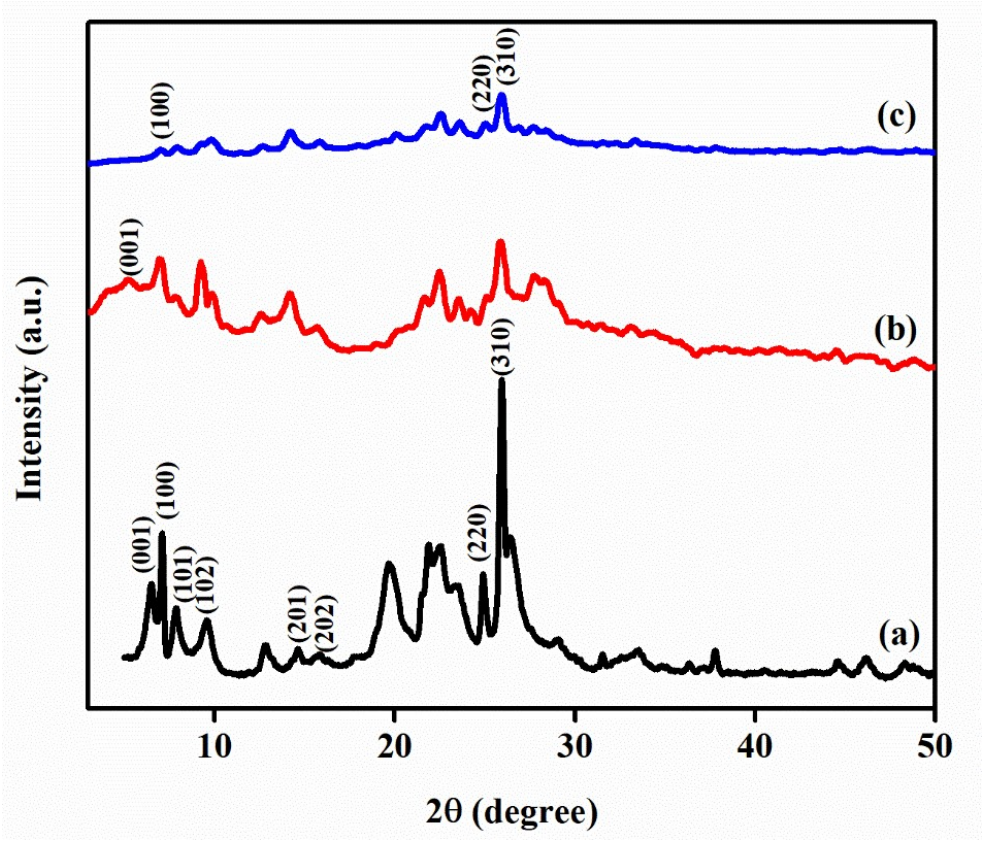

Fig. S1. Powder XRD patterns of (a) MCM-22 (P), (b) MS-1, and (c) ITQ-2.

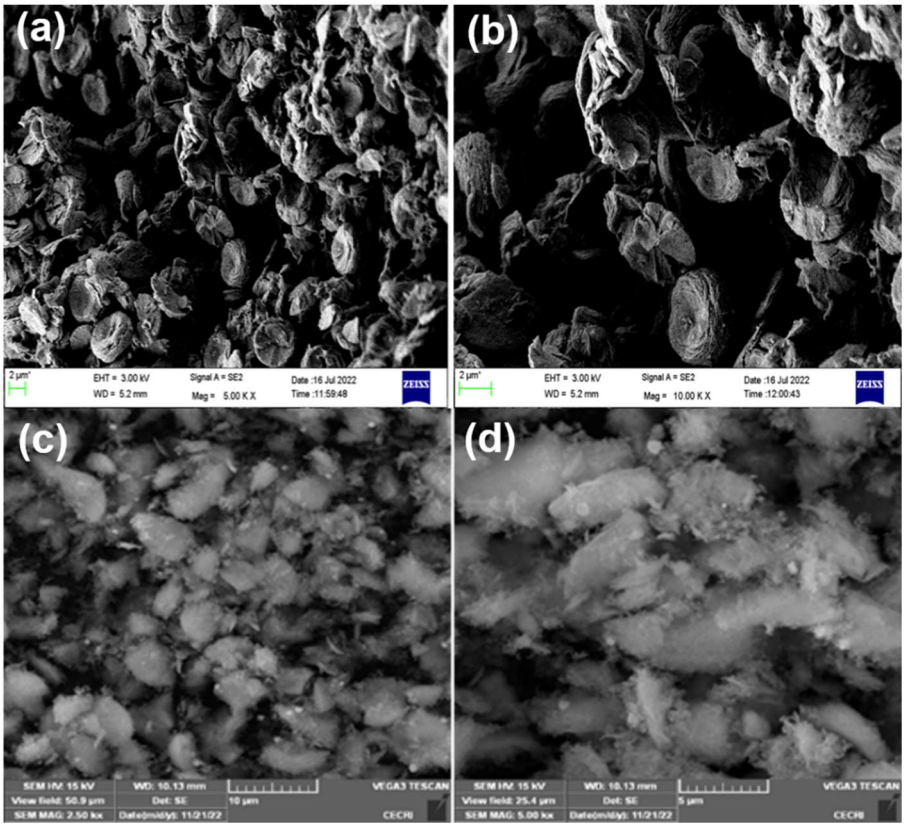

Fig. S2. SEM Images of (a), (b) MS-1, and (c), (d) Ni-ITQ-2 composite (4 mmol Ni).

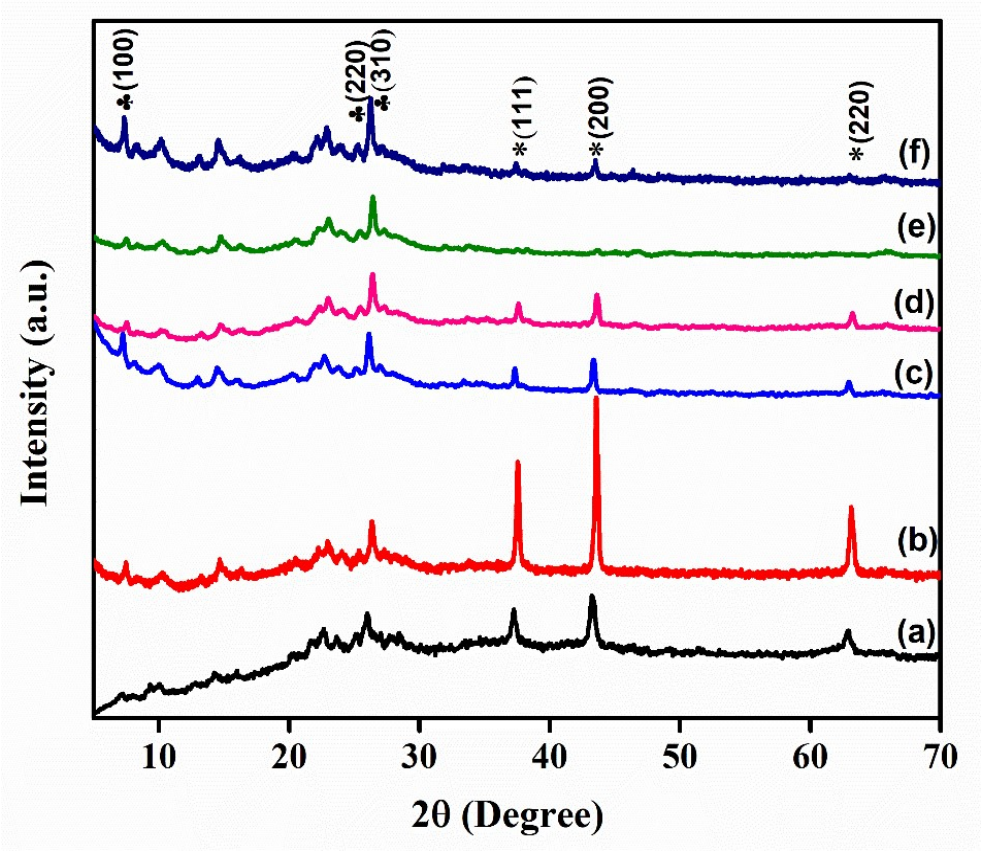

Fig. S3. Powder XRD patterns of Ni-ITQ-2 composite prepared at (a) pH =4, Ni= 4 mmol, (b) pH =2, Ni= 4 mmol, (c) pH =4, Ni= 2 mmol, (d) pH =2, Ni= 2 mmol, (e) pH =4, Ni= 1 mmol, and (f) pH =2, Ni= 1 mmol (♣ represents ITQ-2 peaks and * represents nickel oxide peaks).

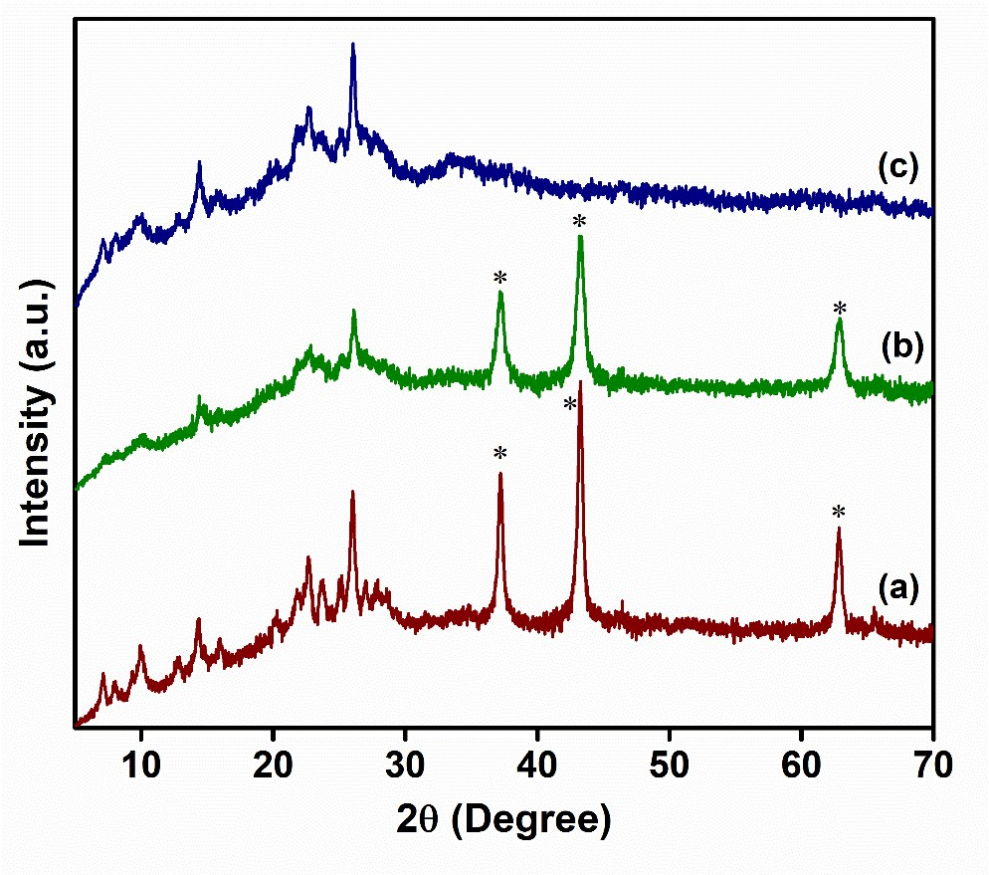

Fig. S4. Powder XRD patterns of (a) Ni-MCM-22, (b) ITQ-2-Ni-W, and (c) Physical mixture of ITQ-2 and NiO (ITQ-2-Ni-P) (* represents nickel oxide peaks).

217

218 Table S2. Unit cell parameters of MCM-22 (P) and Ni-ITQ-2 Composite (4 mmol Ni source).

219

Plane	Sample	2θ	d-spacing (A°)
100	MCM-22 (P)	7.1	12.44
	Without pH adjustment	7.5	11.78
	pH=4	7.2	12.27
	pH=2	7.5	11.78
101	MCM-22 (P)	7.8	11.33
	Without pH adjustment	8.4	10.52
	pH=4	8.1	10.91
	pH=2	8.3	10.64
102	MCM-22 (P)	9.6	9.21
	Without pH adjustment	10.3	8.58
	pH=4	9.9	8.93
	pH=2	10.3	8.58
220	MCM-22 (P)	24.9	3.57
	Without pH adjustment	25.5	3.49
	pH=4	25.2	3.53
	pH=2	25.3	3.52
310	MCM-22 (P)	25.95	3.43
	Without pH adjustment	26.32	3.38
	pH=4	26	3.42
	pH=2	26.35	3.38

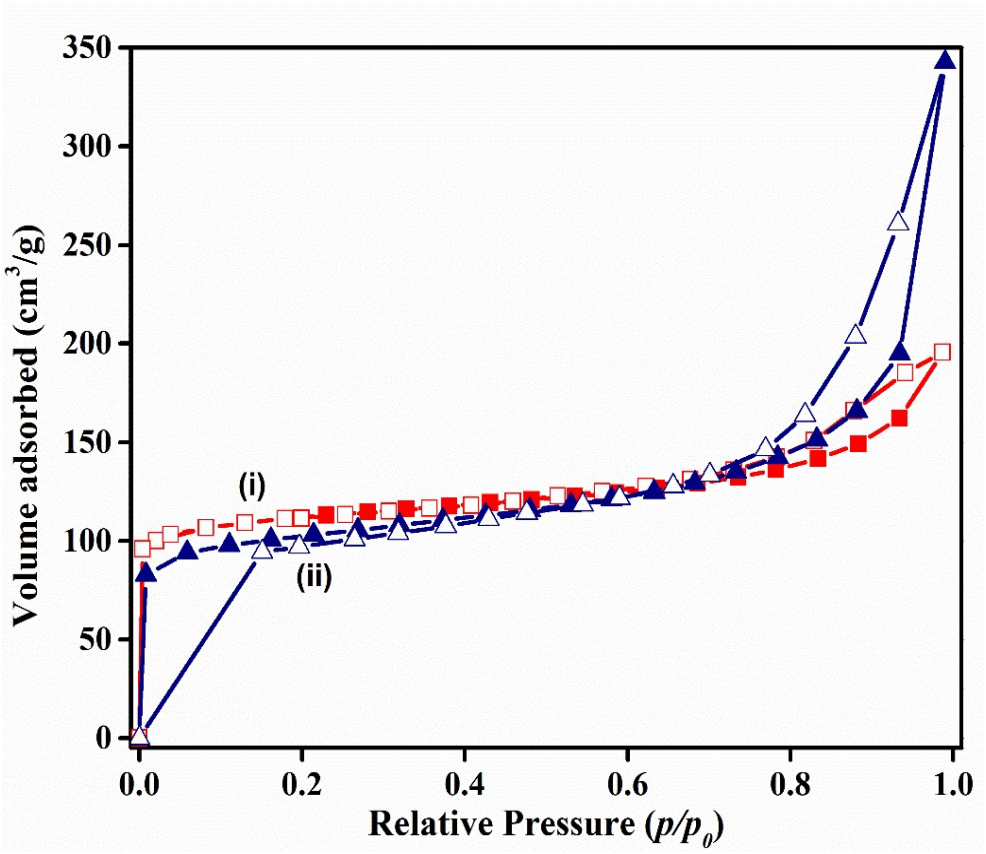

Fig. S5. Nitrogen sorption isotherm of (i) MCM-22, and (ii) ITQ-2.

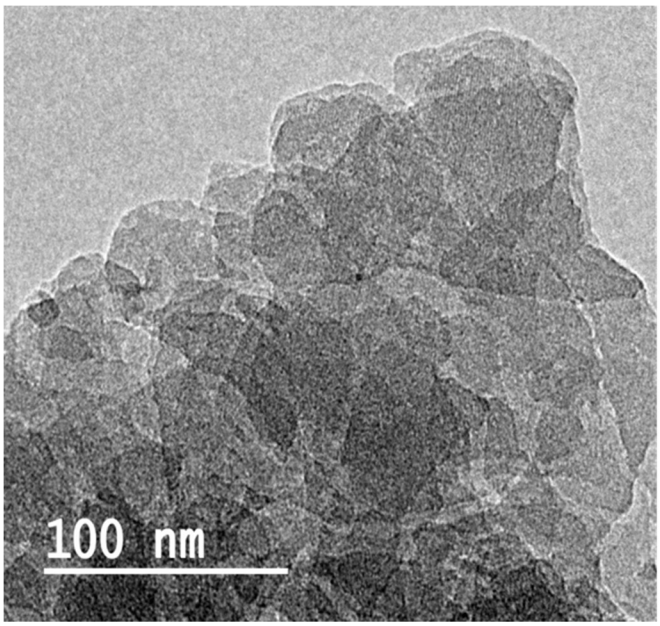

Fig. S6 TEM images of MCM-22 sample.

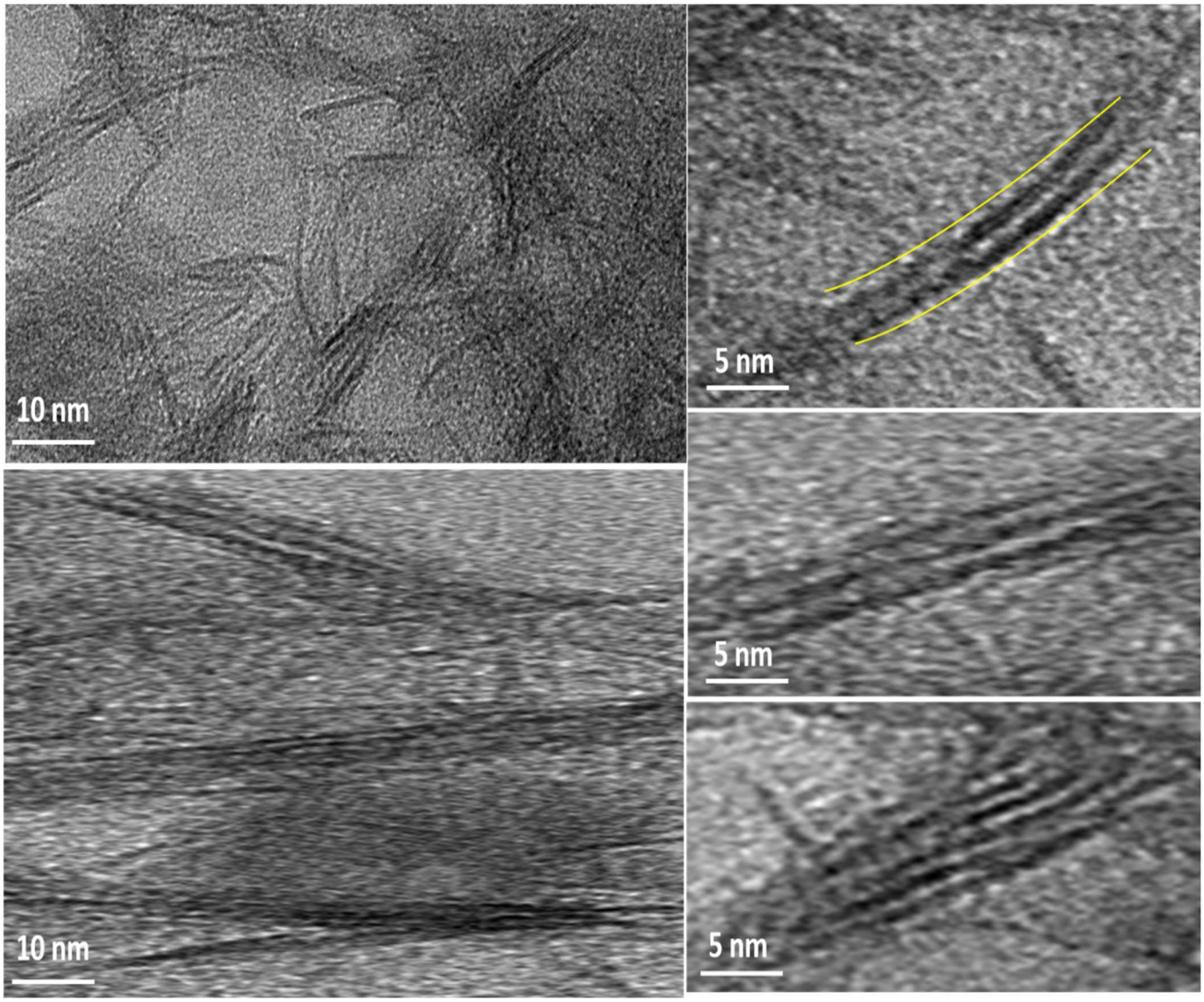

Fig. S7. HR-TEM images of Ni-ITQ-2 composite showing the delaminated ITQ-2 sheets with decorated NiO(OH).

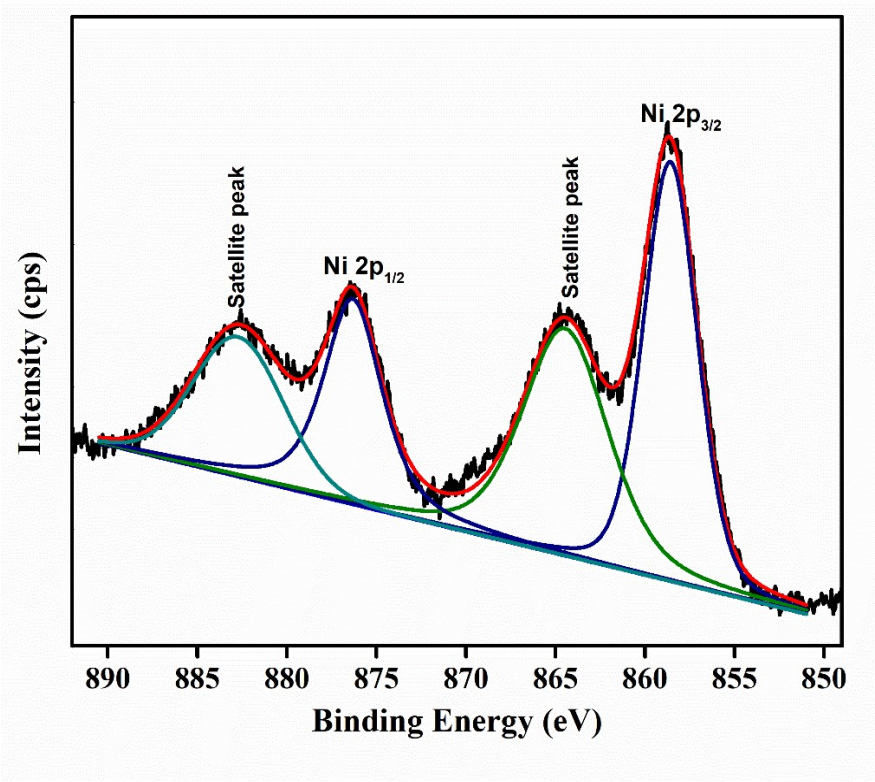

Fig. S8. XPS Profile of Ni 2p in Ni-ITQ-2 composite.

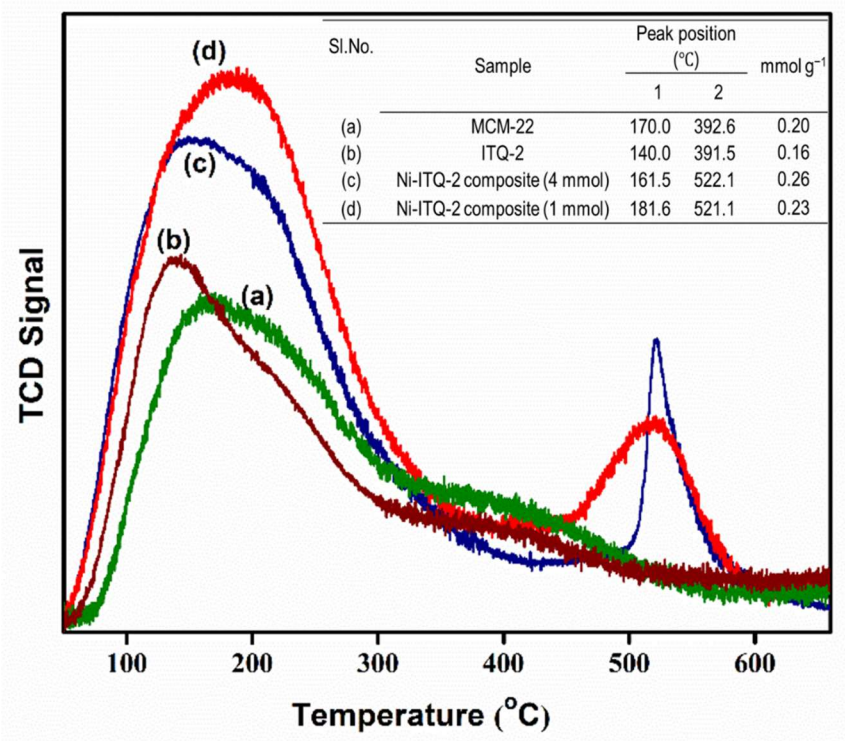

Sl.No.	Sample	Peak position (°C) 1	Peak position (°C) 2	mmol g^{-1}
(a)	MCM-22	170.0	392.6	0.20
(b)	ITQ-2	140.0	391.5	0.16
(c)	Ni-ITQ-2 composite (4 mmol)	161.5	522.1	0.26
(d)	Ni-ITQ-2 composite (1 mmol)	181.6	521.1	0.23

Fig. S9. Ammonia temperature programmed desorption profile of (a) MCM-22, (b) ITQ-2, and Ni-ITQ-2 composite prepared with Ni concentration of (c) 4 mmol, and (d) 1 mmol.

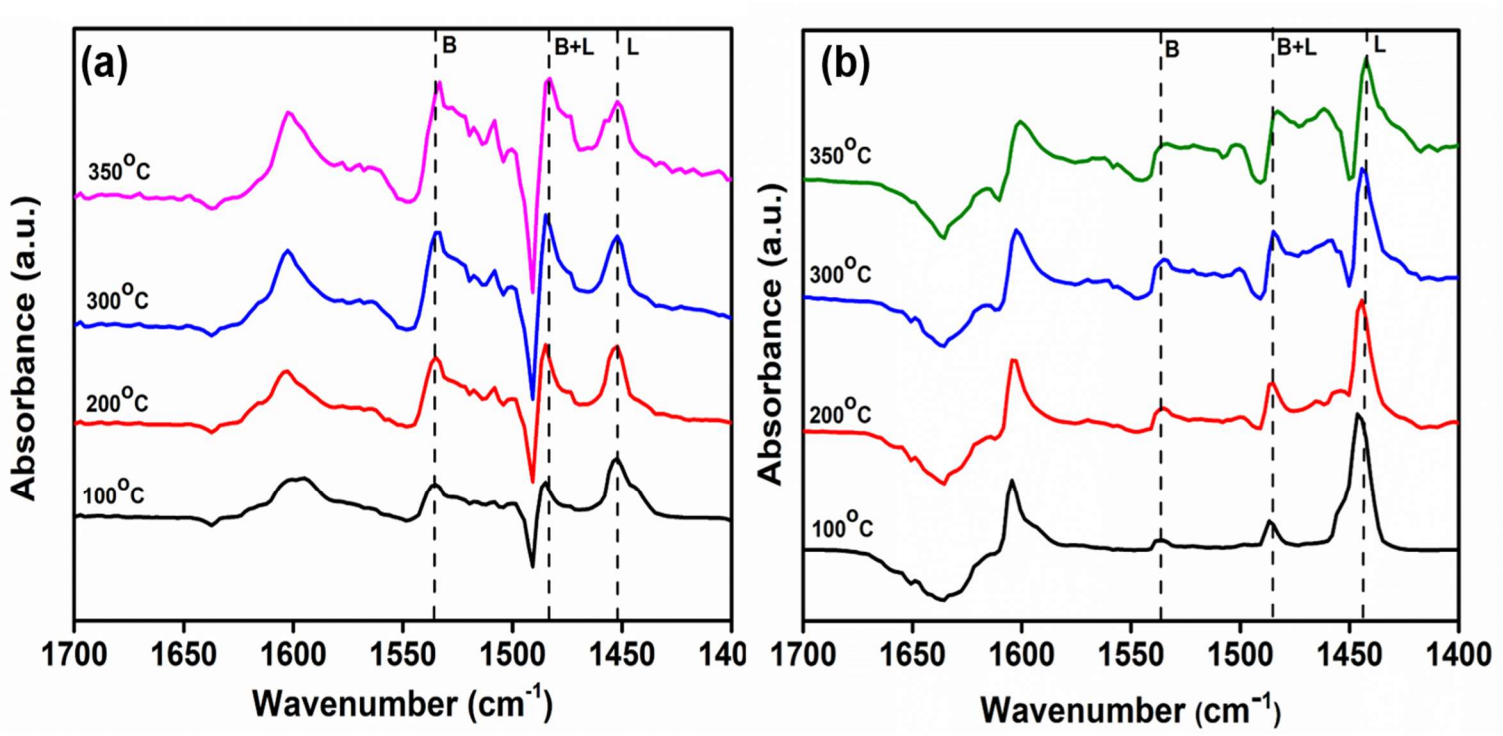

Fig. S10. IR Pyridine desorption spectra of (a) MCM-22, and (b) Ni-ITQ-2 composite.

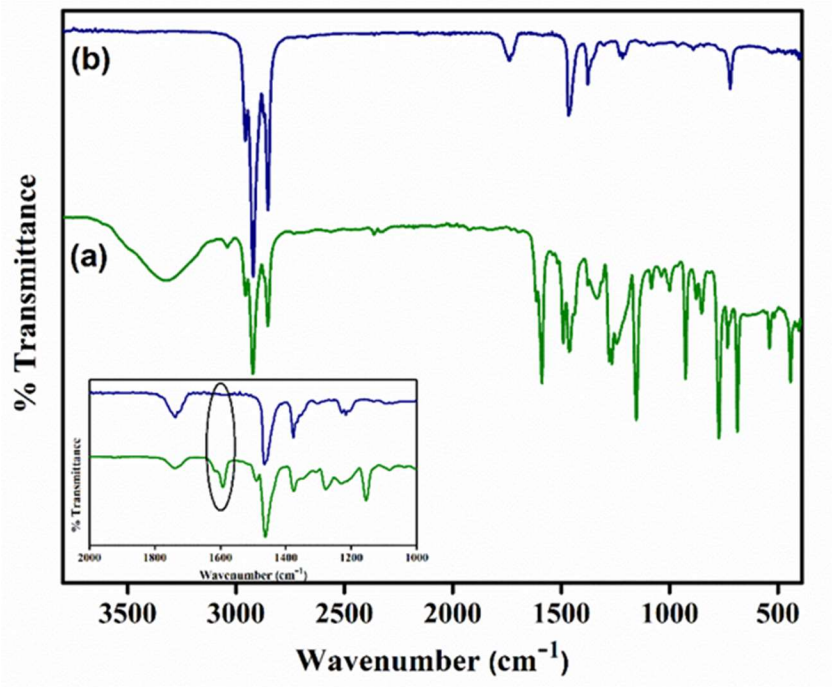

Fig. S11. FTIR spectra of (a) Reaction and (b) Product mixture of *m*-cresol HDO processes.

XXXX Report

Printing time: Thu Apr 20 15:21:35 2023
Injection time: Thu Apr 20 12:50:01 2023

File opened: D:\Old Files\Nimisha\HP88\m-cresolHDO\Ni-ITQ-2 comp\ Reaction mixture;m-cresol and DD.hw

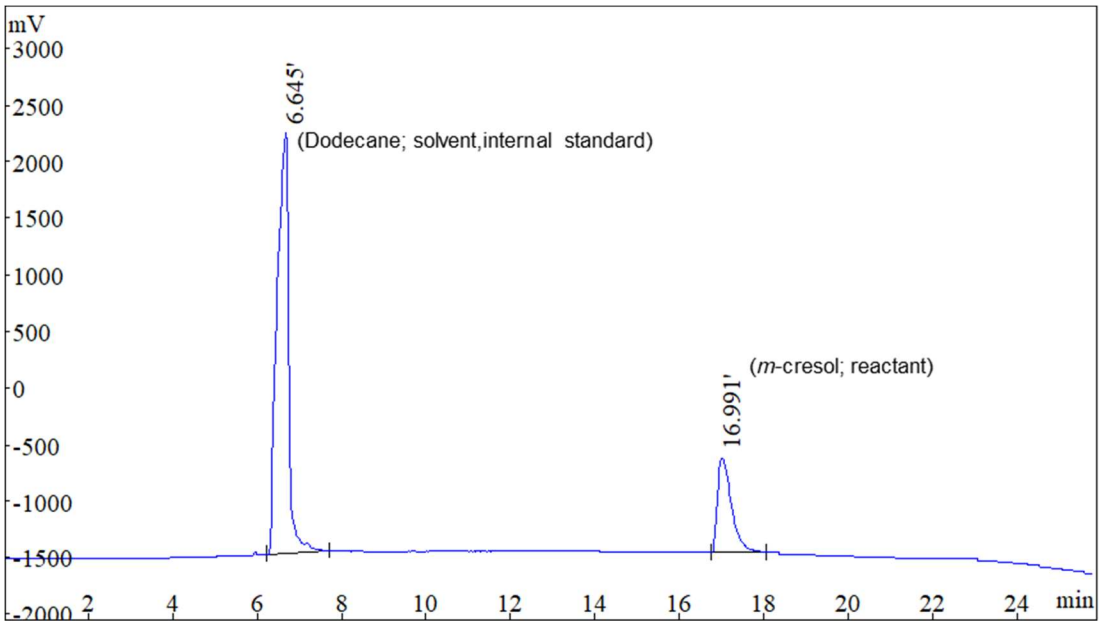

Rank	Time	Name	Area%	Area
1	6.645		78.88	67427891
2	16.991		21.12	18056621
Total			100	85484512

Fig. S12. GC pattern of the starting reaction mixture.

XXXX Report

Printing time: Thu Apr 20 16:52:17 2023
Injection time: Thu Jul 20 14:59:48 2023

File opened: D:\Old Files\Nimisha\HP88\m-cresol HDO\Ni-ITQ-2 comp\DD,cresol,methylcyclohexane.hw

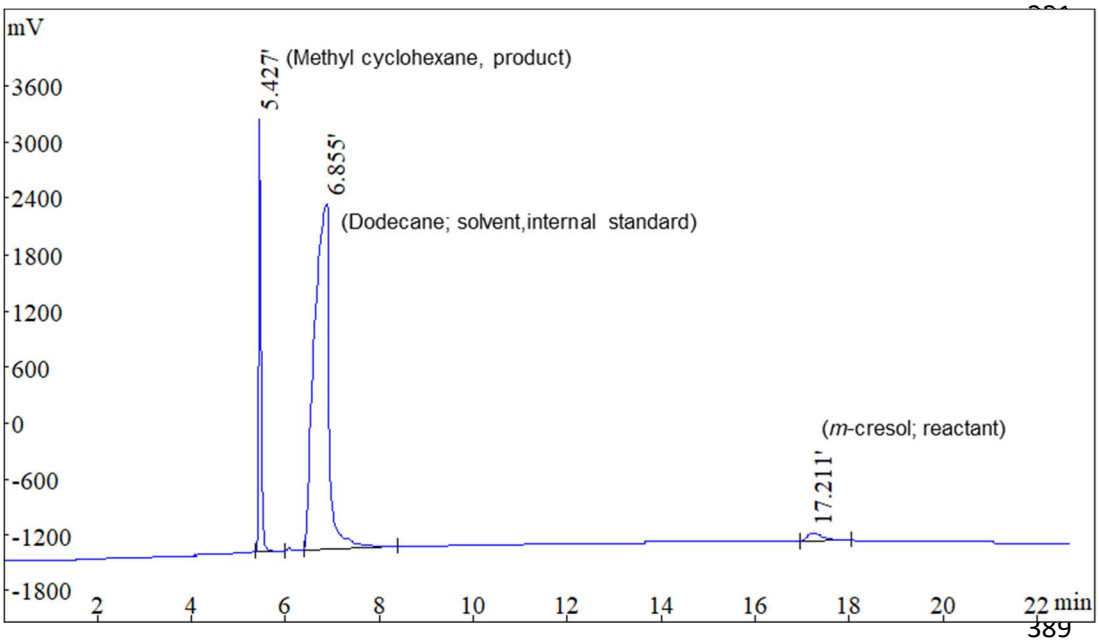

Rank	Time	Name	Area%	Area
1	5.427		13.03	11823204
2	6.855		84.89	77058227
3	17.211		2.085	1892803
Total			100	90774234

Fig. S13. GC pattern of the product mixture.

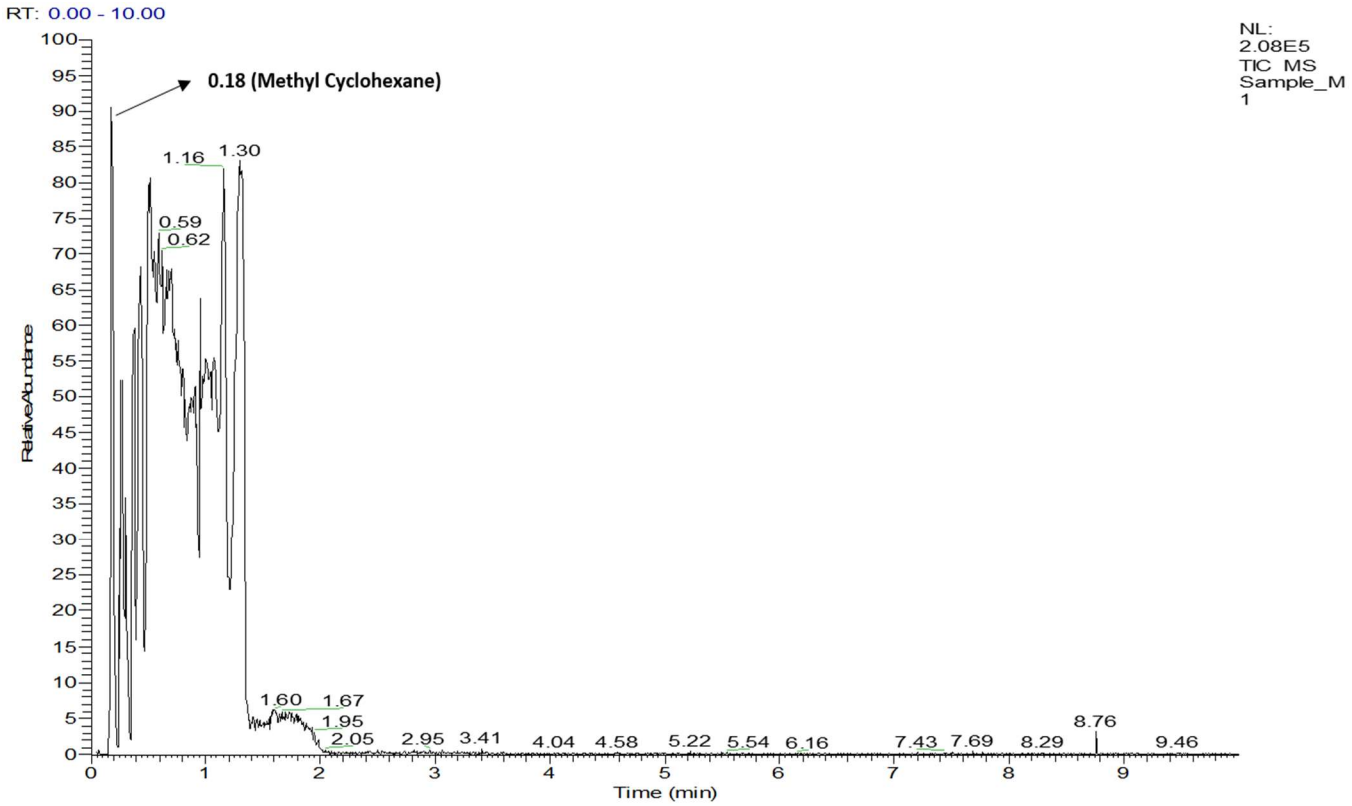

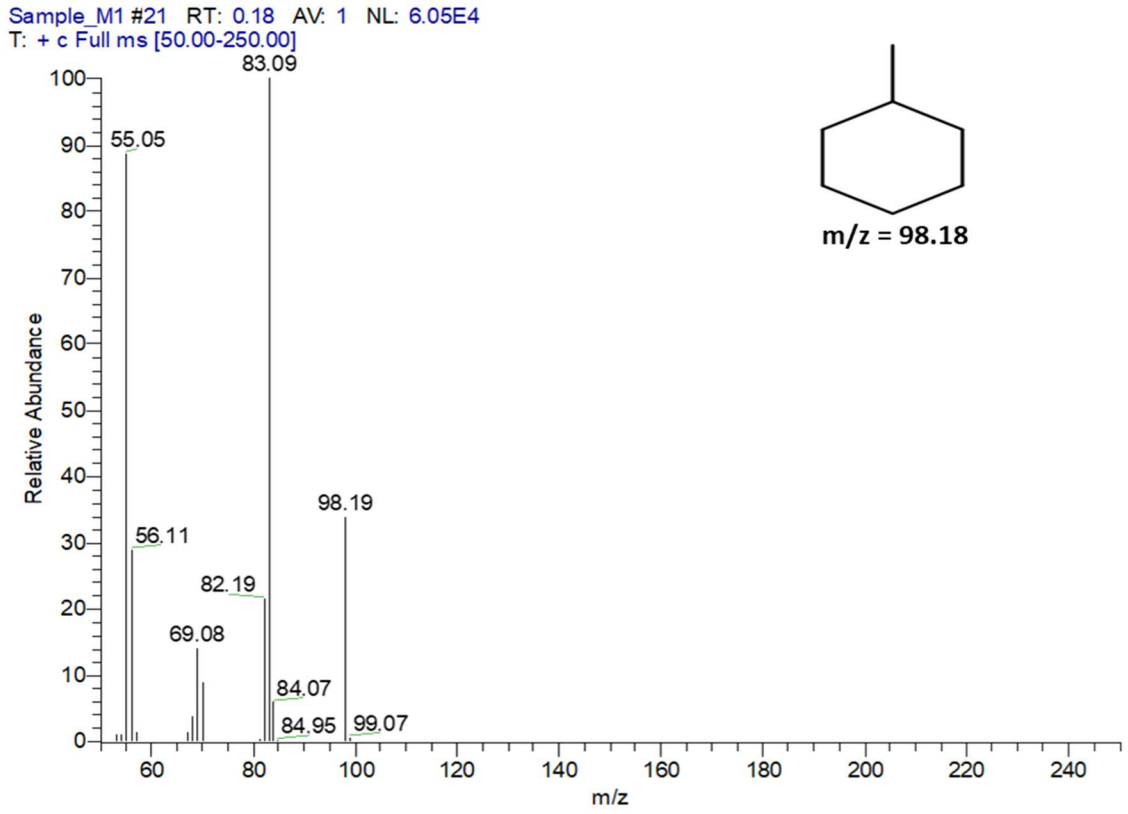

Fig. S14. GC-MS chromatogram of exclusive hydrodeoxygenated product, viz., methyl cyclohexane.

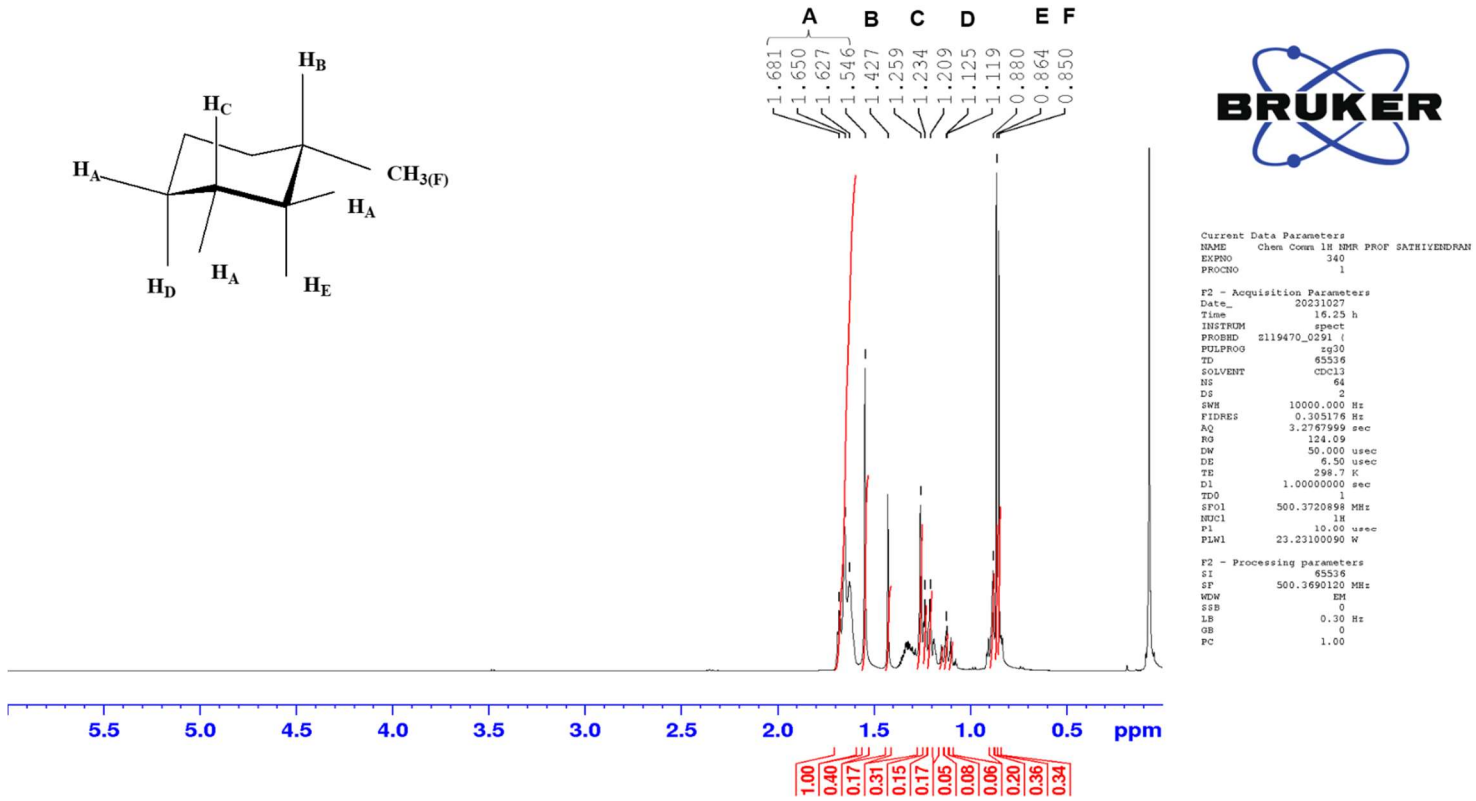

Fig. S15 ^{1}H NMR of exclusive hydrodeoxygenated product, viz., methyl cyclohexane;(Additional peaks are due to the presence of trace amount of *n*-dodecane; solvent used in *m*-cresol HDO reaction)[2].

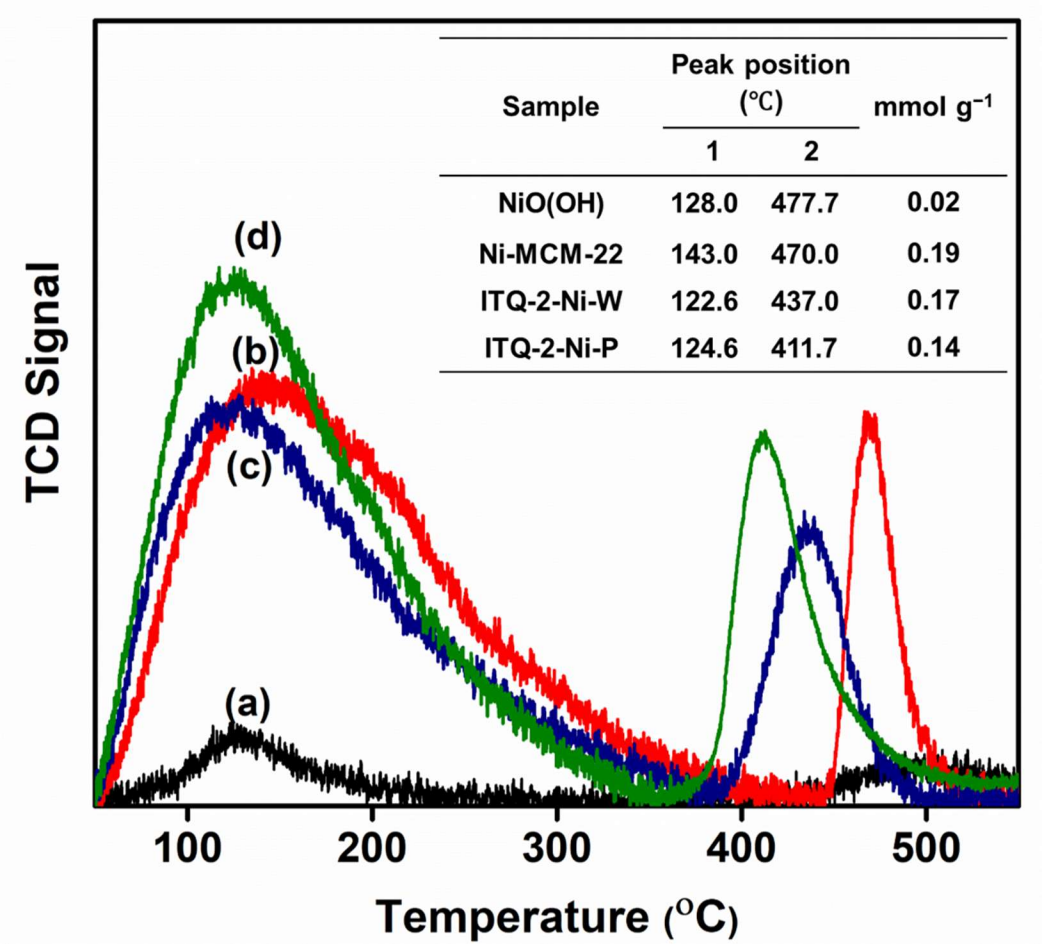

Sample	Peak position (°C)		mmol g^{-1}
	1	2	
NiO(OH)	128.0	477.7	0.02
Ni-MCM-22	143.0	470.0	0.19
ITQ-2-Ni-W	122.6	437.0	0.17
ITQ-2-Ni-P	124.6	411.7	0.14

Fig. S16. Ammonia temperature programmed desorption profile of (a) NiO(OH), (b) Ni-MCM-22, (c) ITQ-2-Ni-W, and (d) ITQ-2-Ni-P.

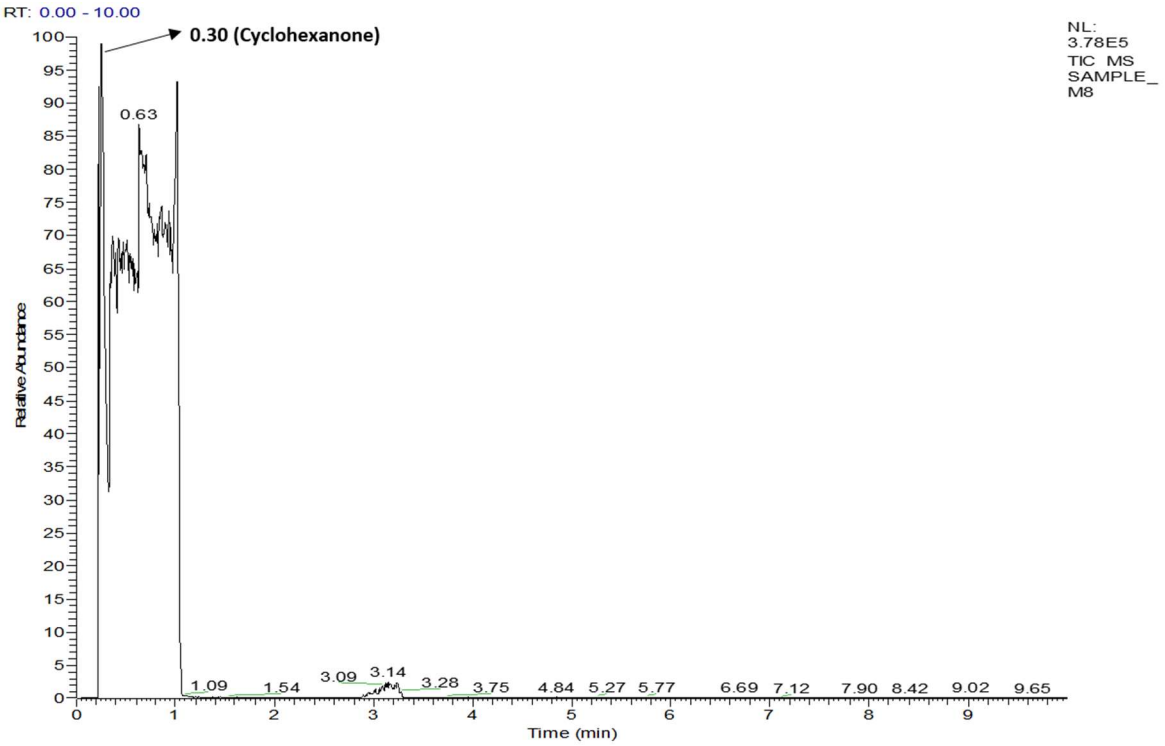

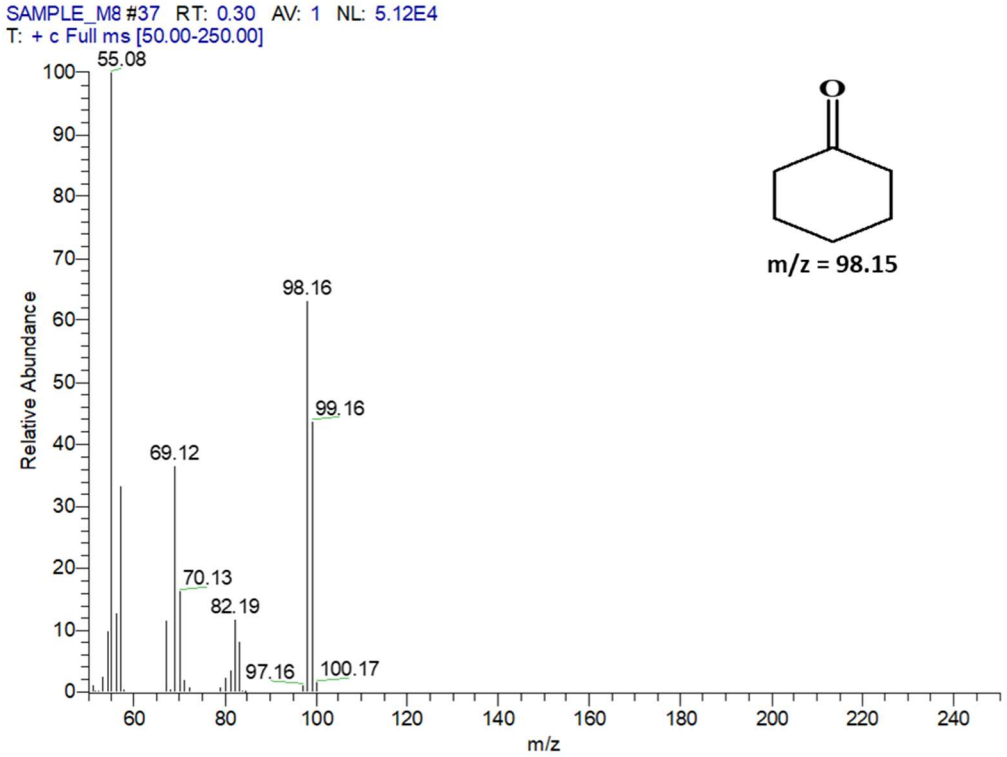

Fig. S17. GC-MS chromatogram of cyclohexanone (intermediate product in HDO).

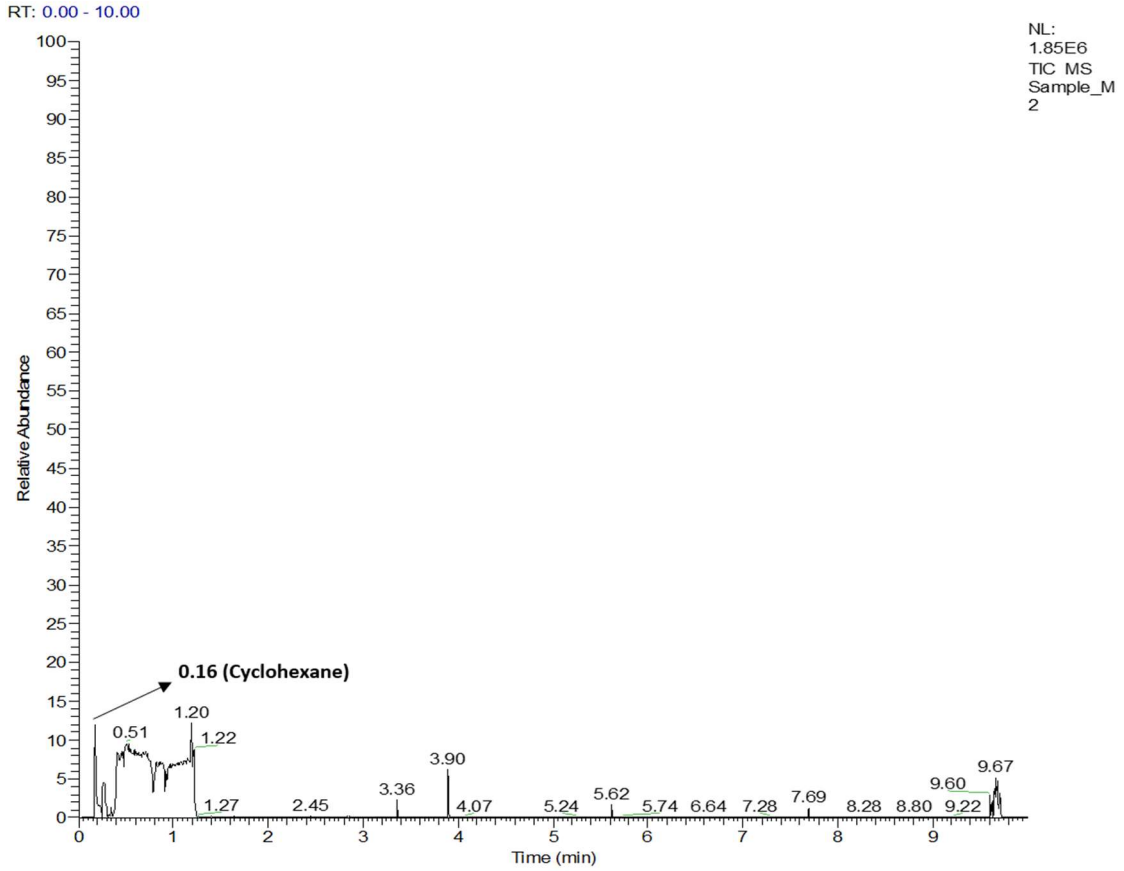

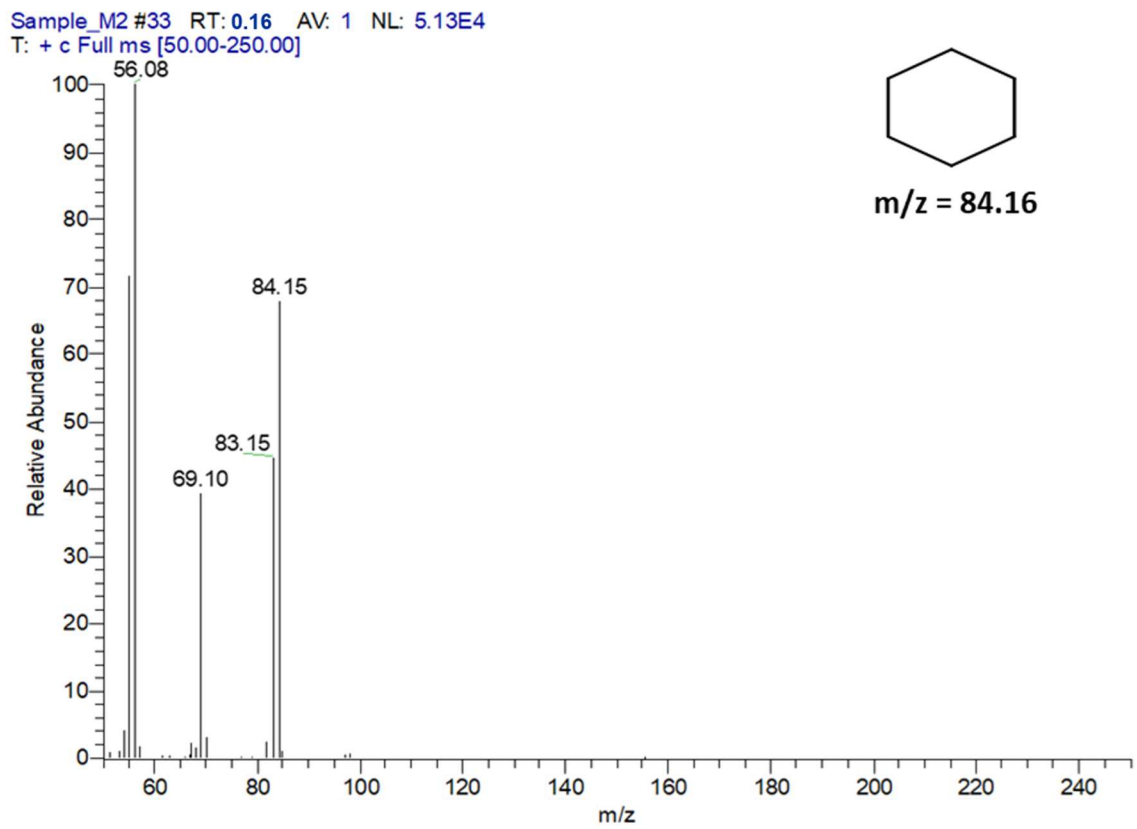

Fig. S18. GC-MS chromatogram of hydro-deoxygenated product of phenol.

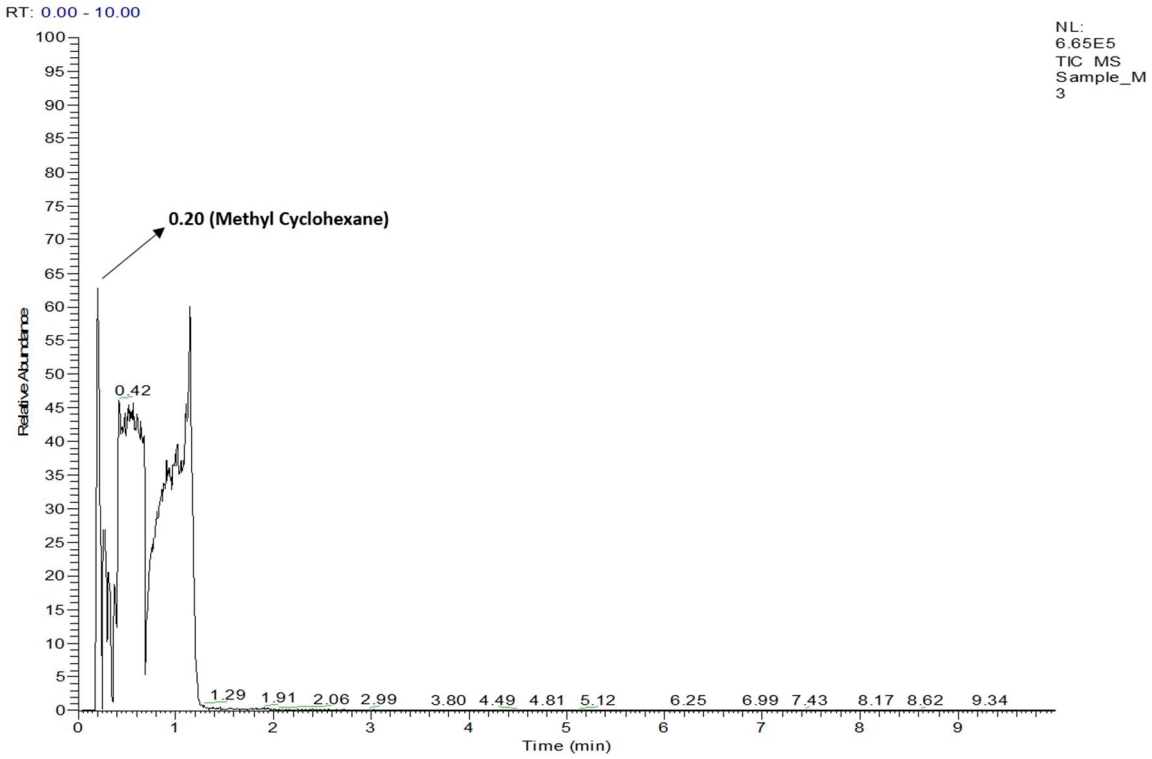

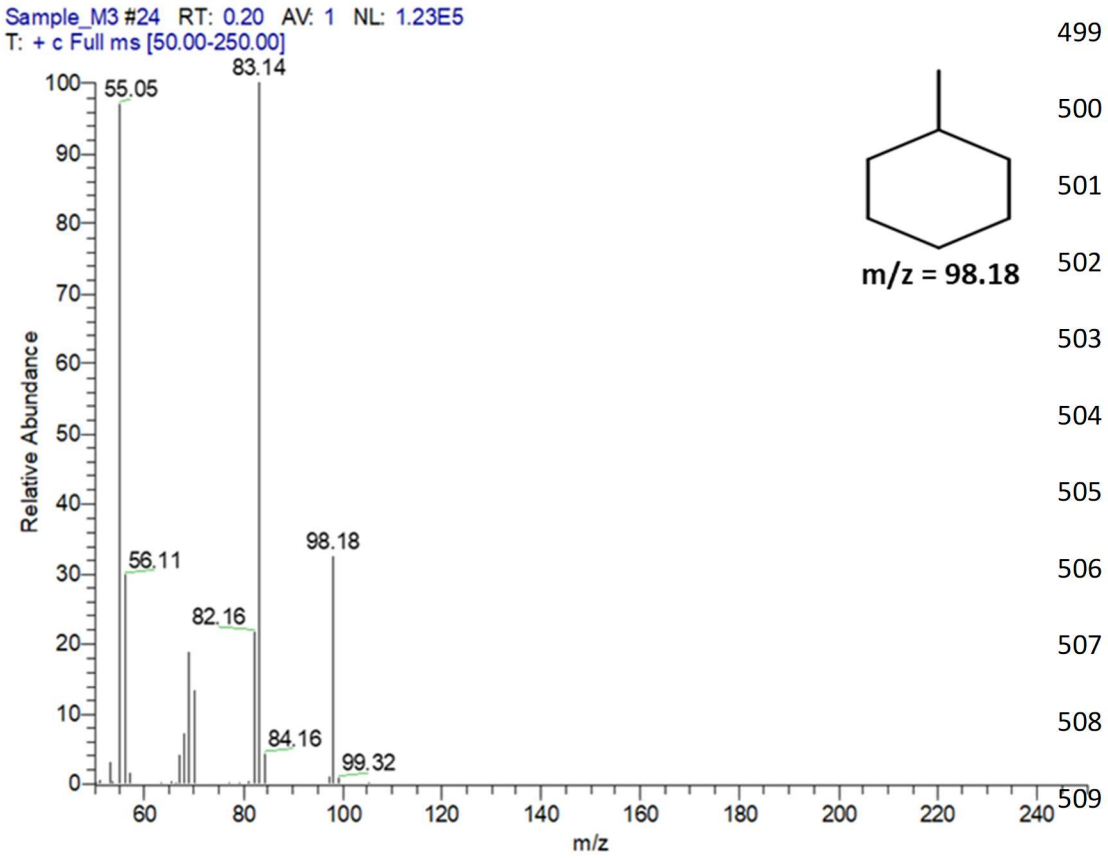

Fig. S19. GC-MS chromatogram of hydrogenated product of toluene.

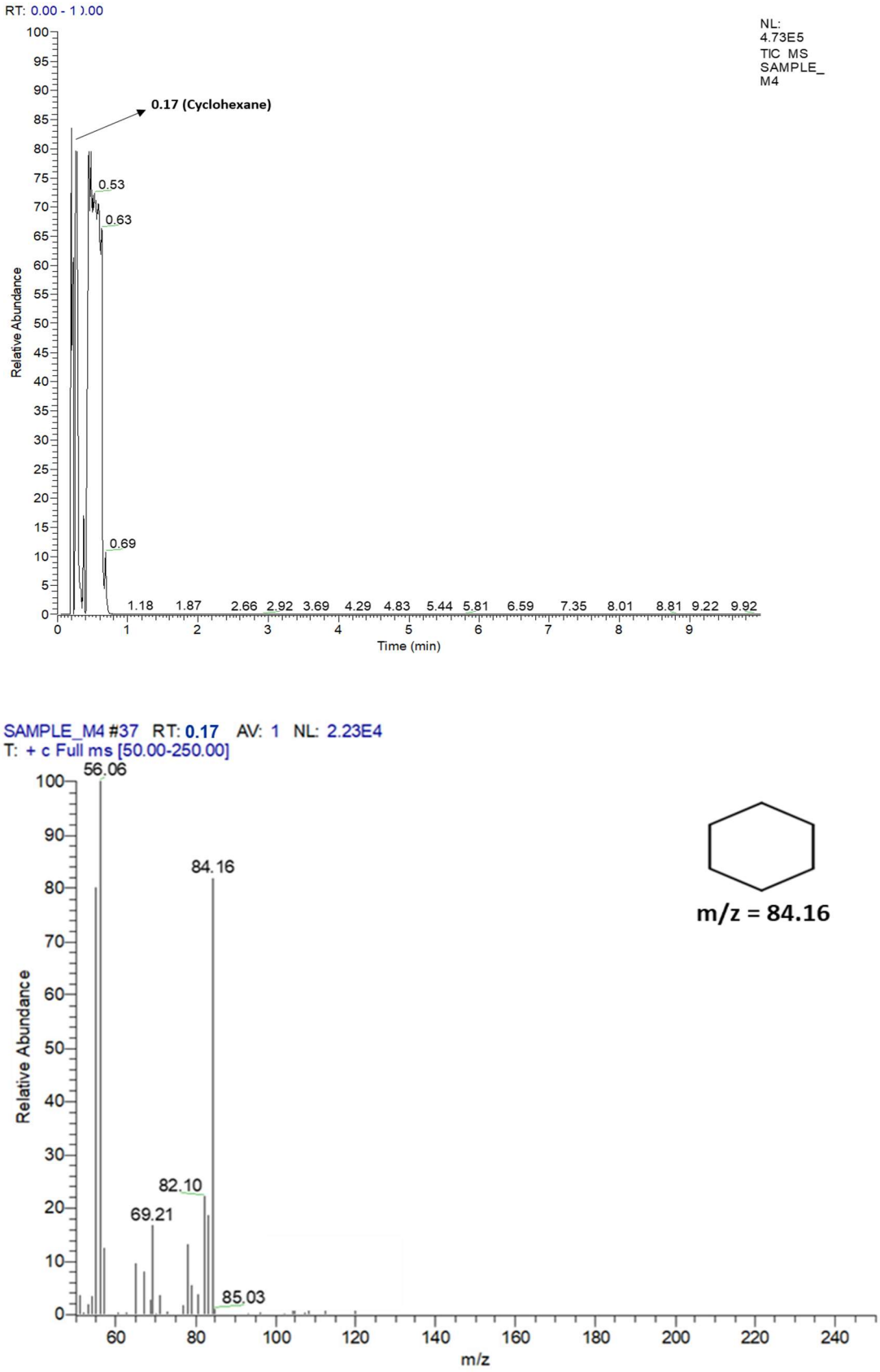

Fig. S20. GC-MS chromatogram of hydrodeoxygenated product of anisole.

Sample Header

Data File:	s5
Original Data Path:	H:\data\DGN
Sample Name:	
Dr. D. Tripathi	deependra
Comments:	

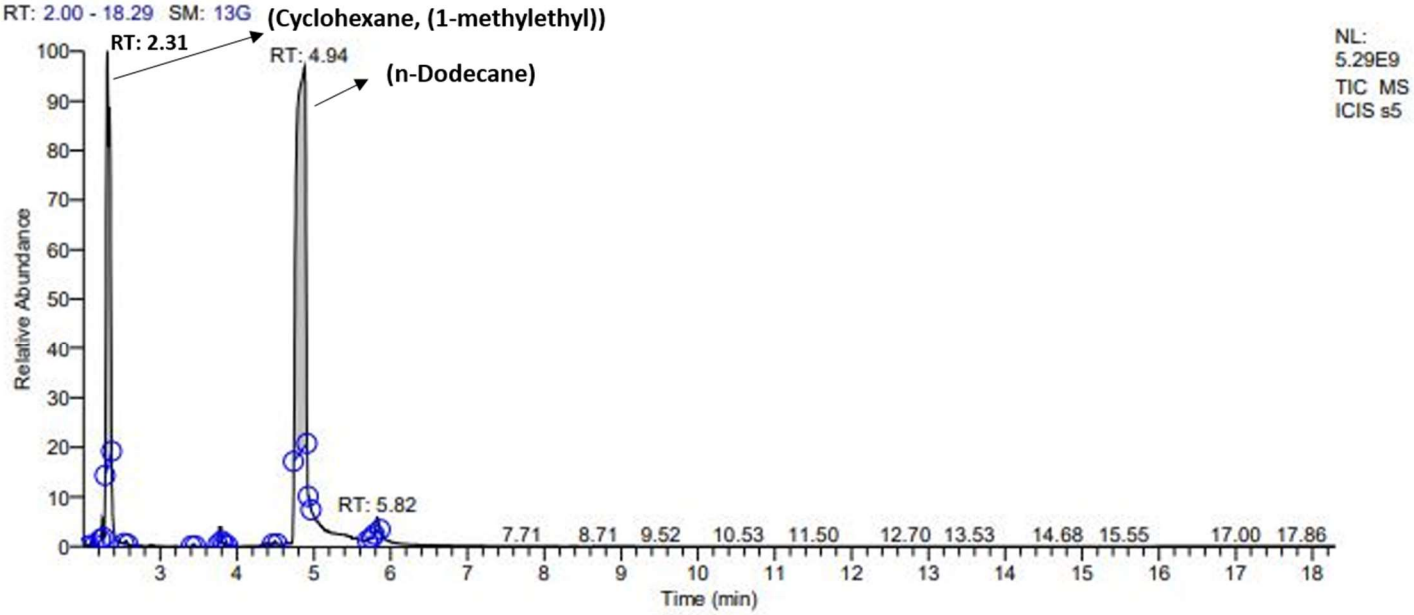

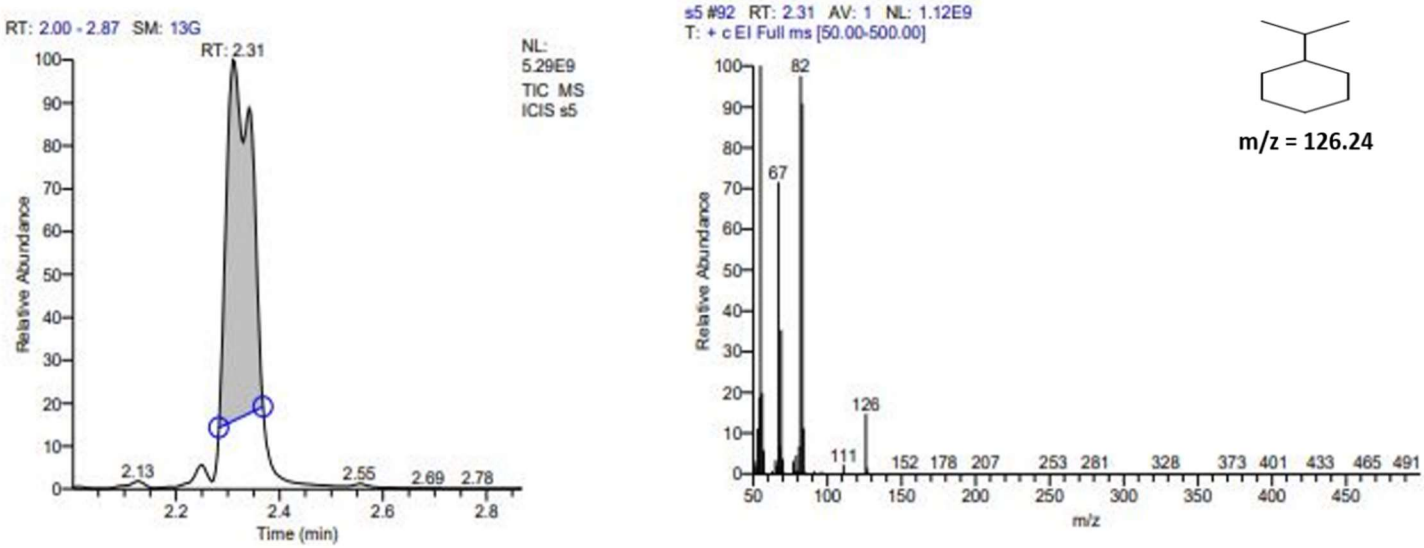

Fig. S21. GC-MS chromatogram of hydrogenated product of cumene.

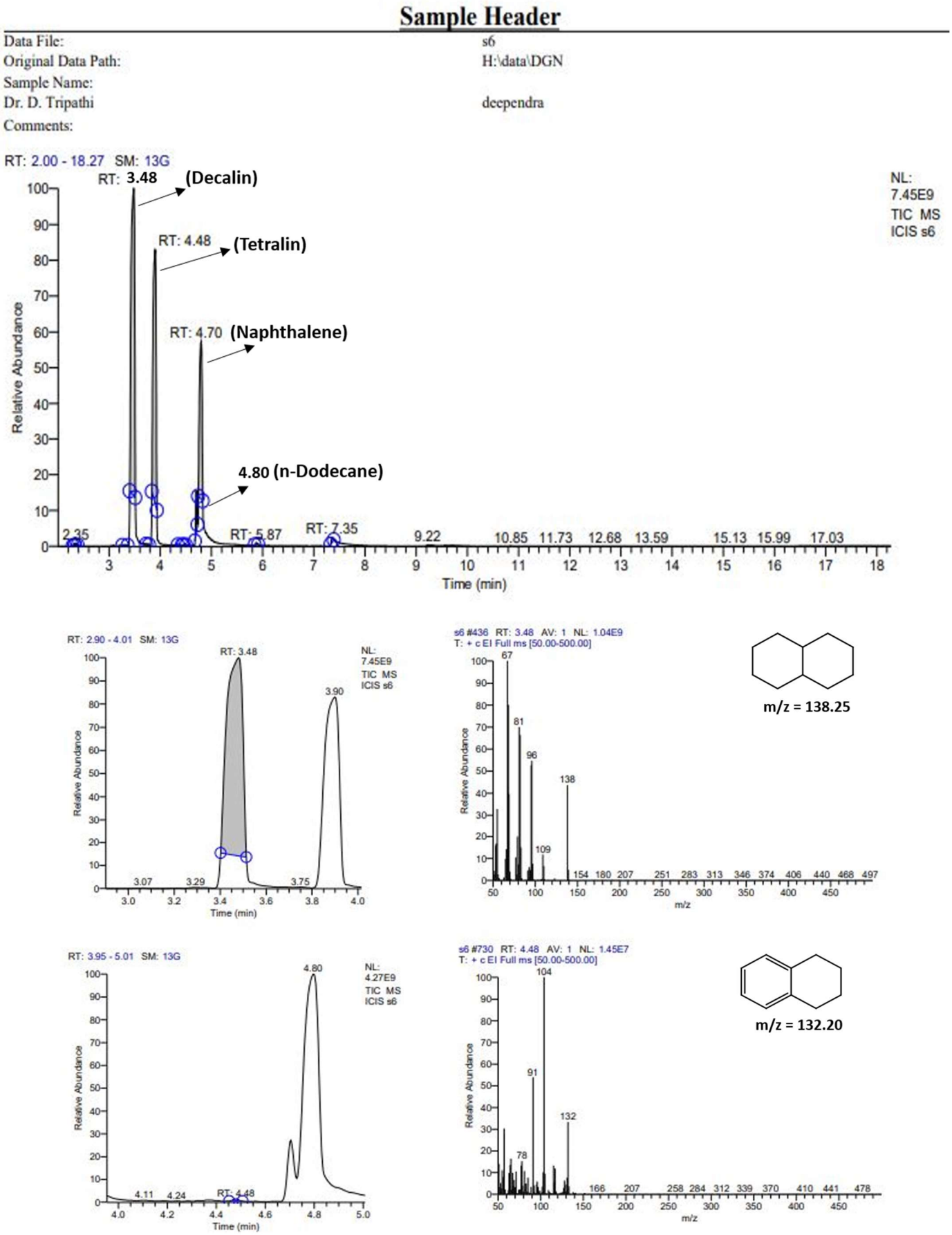

Fig. S22. GC-MS chromatogram of hydrogenated product of naphthalene.

XXXX Report

Printing time: Tue Nov 28 10:24:58 2023
Injection time: Fri Nov 24 11:03:18 2023

File opened: D:\Old Files\Nimisha\HP88\m-cresol\m-cresol after column cut\M 100 GAS REP.hw

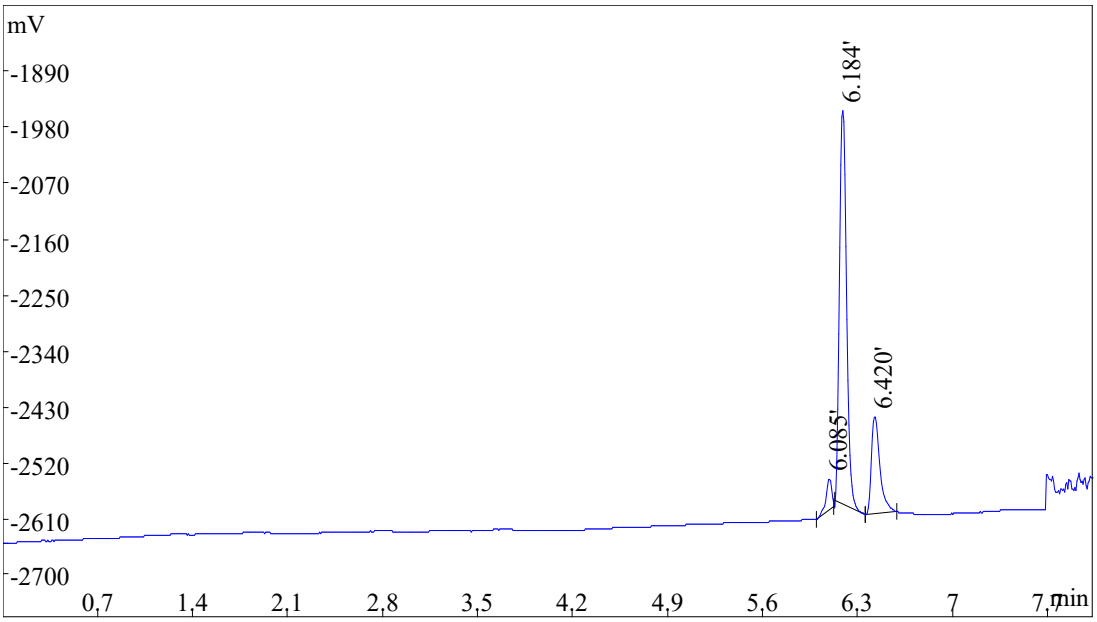

Rank	Time	Name	Area%	Area
1	6.085		4.673	130648
2	6.184		73.03	2041588
3	6.420		22.3	623523
Total			100	2795759

Fig. S23. GC pattern showing the gas product containing methanol in anisole HDO.

XXXX Report

Printing time: Tue Nov 28 10:29:44 2023
Injection time: Sat Nov 25 11:40:14 2023

File opened: D:\Old Files\Nimisha\HP88\m-cresol\m-cresol after column cut\M 100 LIQ.hw

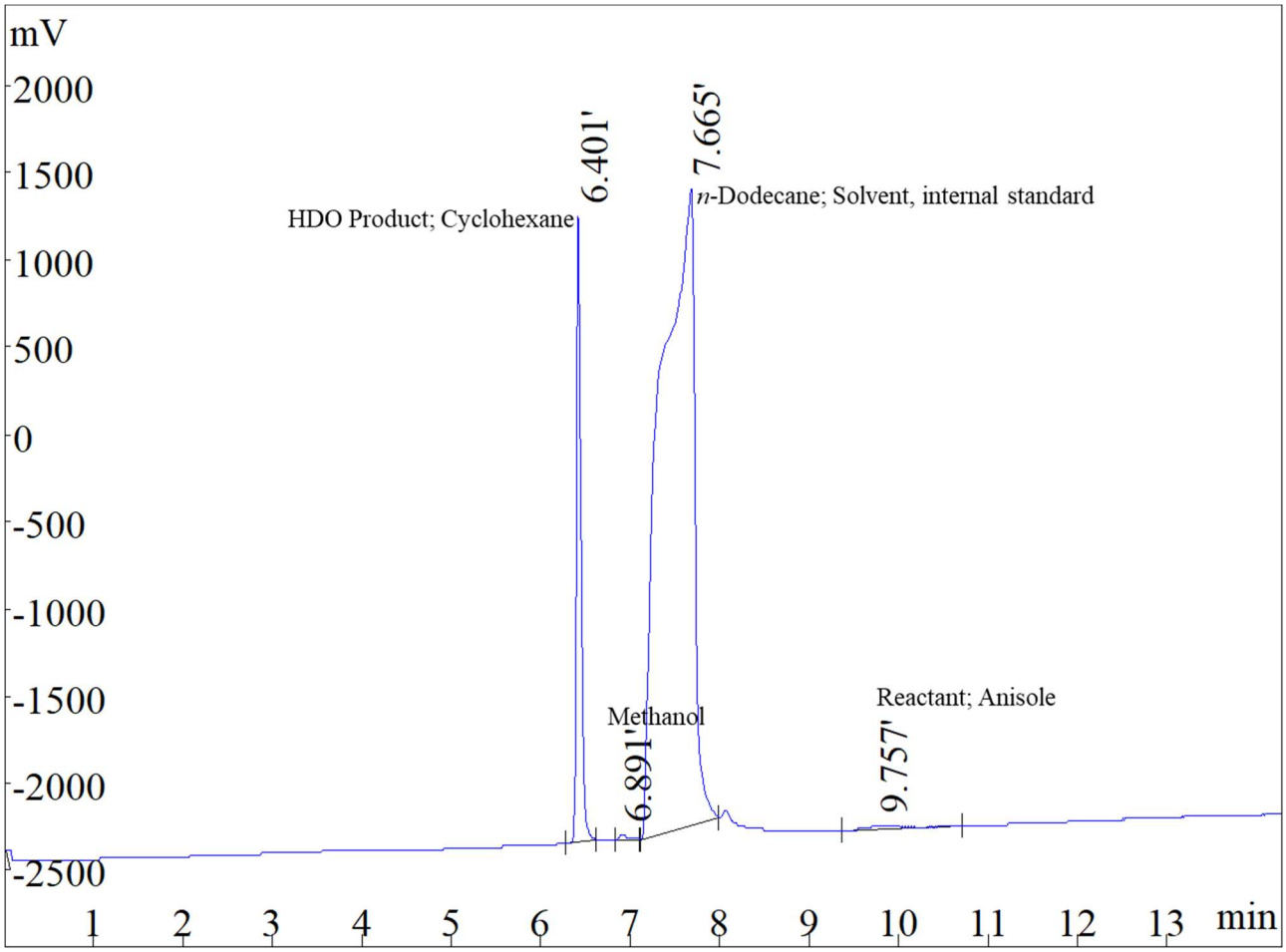

Rank	Time	Name	Area%	Area
1	6.401		9.84	9993574
2	6.891		0.1741	176774
3	7.665		89.53	90926227
4	9.757		0.4564	463565
Total			100	101560140

Fig. S24. GC pattern showing the liquid product of anisole HDO.

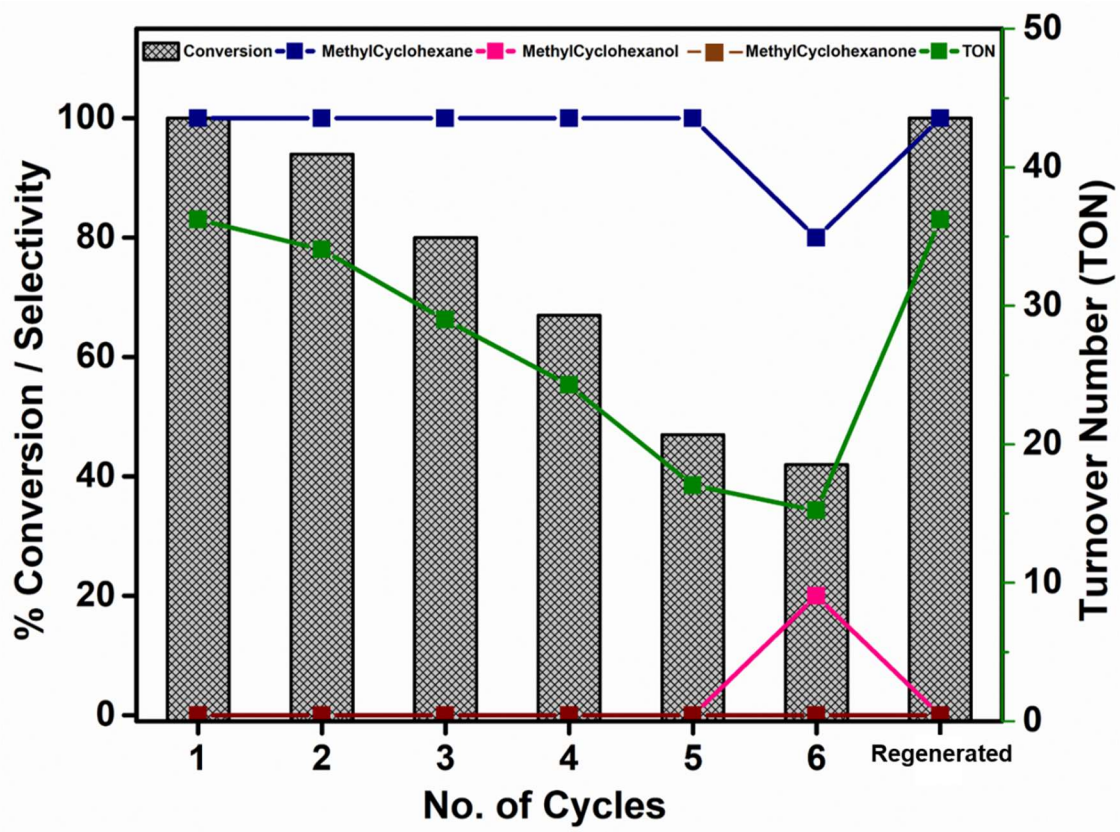

Fig. S25. Recyclability studies over Ni-ITQ-2 composite (Reaction conditions: *m*-cresol-2 mmol, T = 170 °C, t = 6 h, Pressure-2 MPa, Solvent = *n*-dodecane).

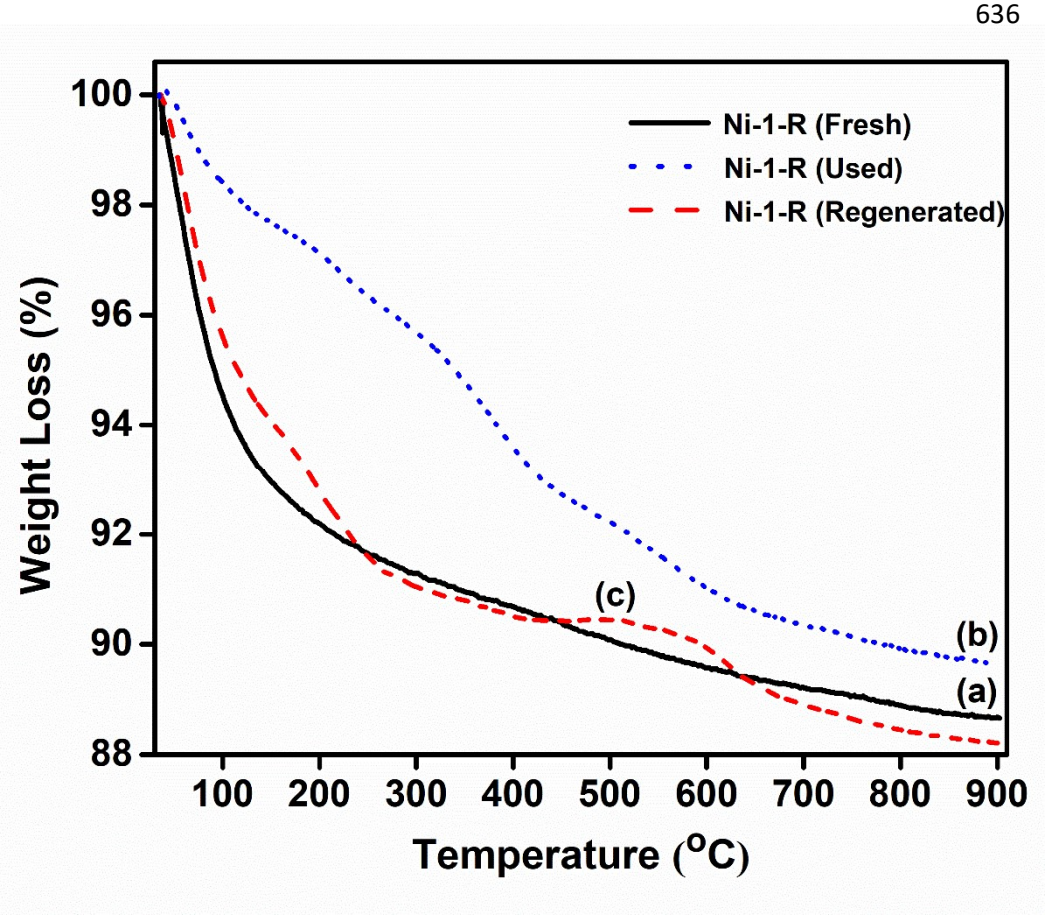

Fig. S26. TGA Profile of (a) Fresh Ni-ITQ-2 composite, (b) Used Ni-ITQ-2 composite, and (c) regenerated Ni-ITQ-2 composite.

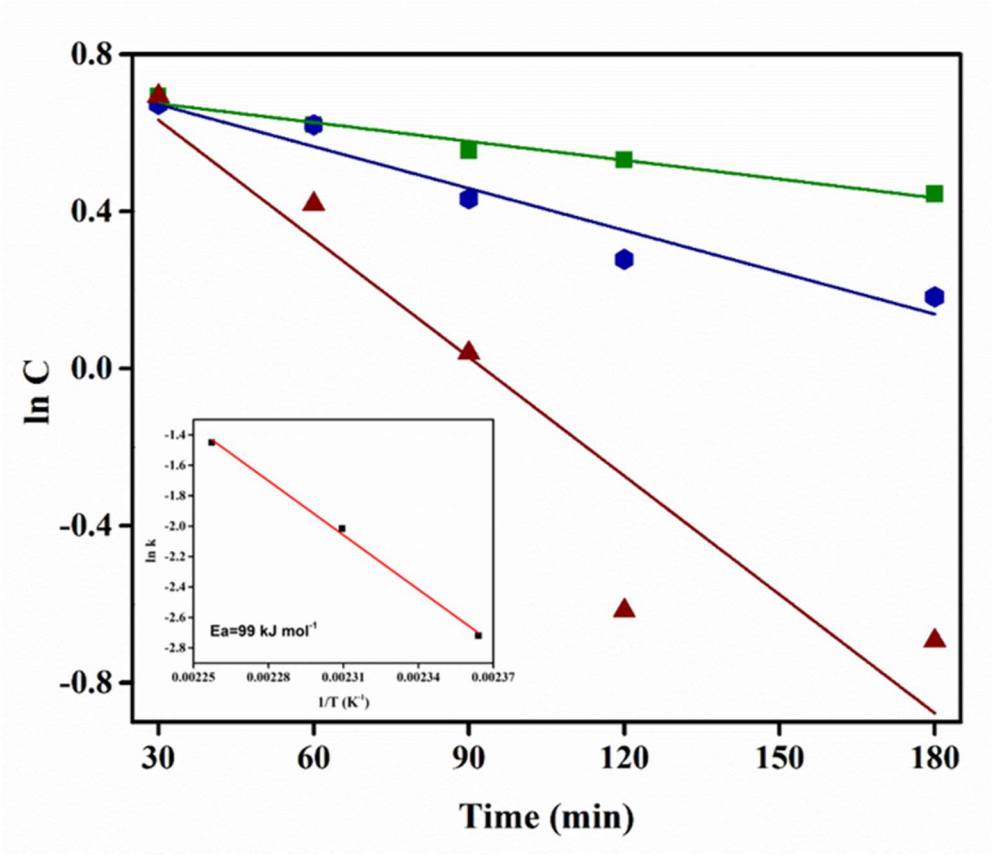

Fig. S27. The concentration of *m*-cresol as a function of time at various reaction temperature over Ni-ITQ-2 composite, and the inset figure showed the Arrhenius plot derived from kinetics data.

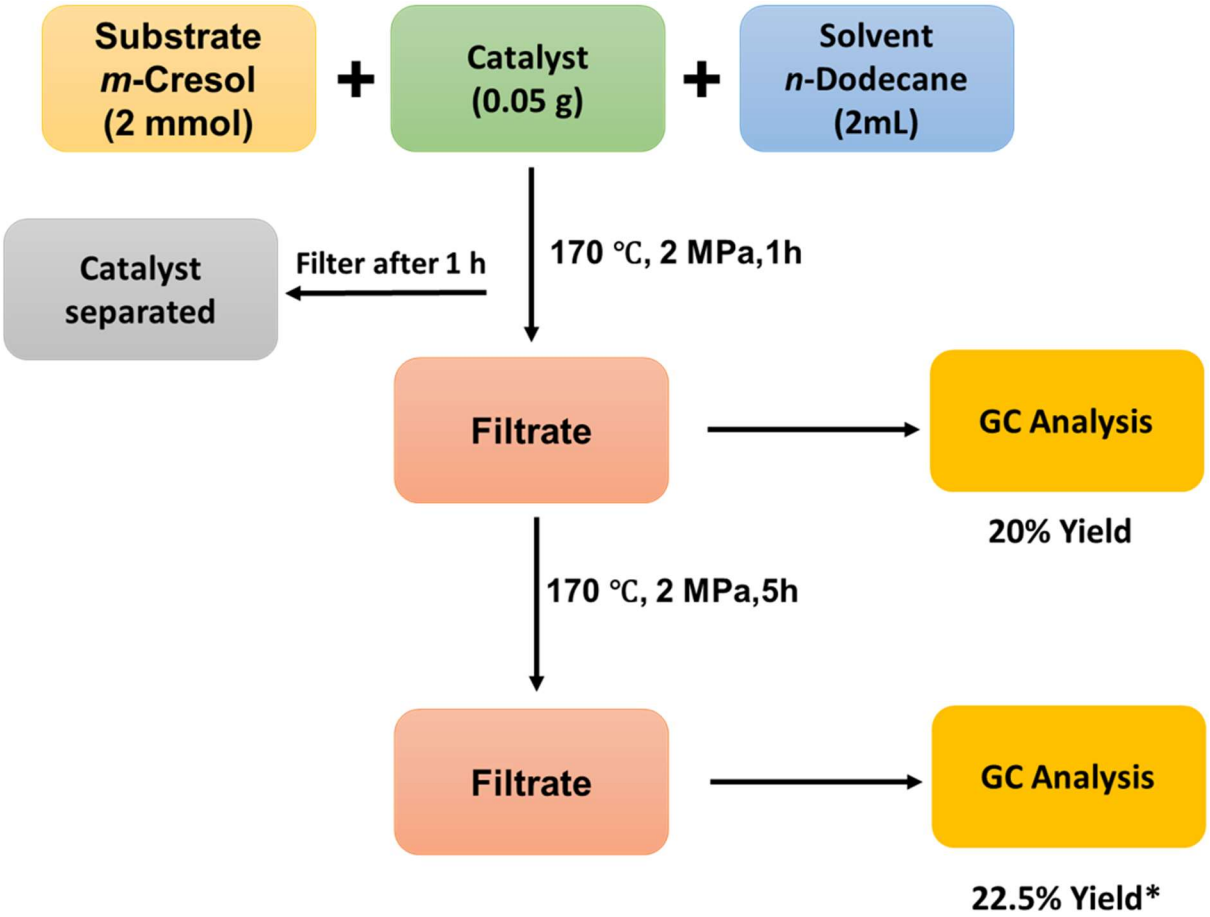

(*:Original yield = 20%, Yield after quenching studies = 22.5%. Therefore, the yield due to activity in filtrate solution = 2.5%)

Fig. S28. Scheme representation for the hot filtration test.

715

716

717 Table S3: N_2 Sorption analysis summary of Ni-ITQ-2 composite.

718

719

Catalyst	**Surface Area (m^2/g)**	**Pore Volume (cm^3/g)**
	BET	BJH
MS-1	380	0.43
ITQ-2	409	0.21
Ni (No pH adjustment, 4 mmol)	332	0.47
Ni (pH=4, 4 mmol)	355	0.56
Ni (pH=2, 4 mmol)	363	0.39
Ni (pH=2, 2 mmol)	388	0.62
Ni (pH=2, 1 mmol)	444	0.36

720

721

722

723

724

725

726

727

728

729

Table S4. Hydro-treating of various aromatic substrates on Ni-ITQ-2 composite catalyst.

Substrate	% Conversion	Major Product	Turnover Number
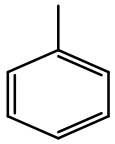	98	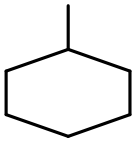	36
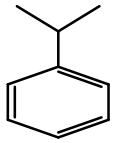	54	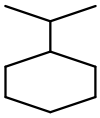	20
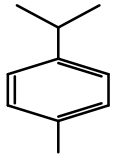	79	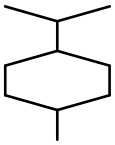	29
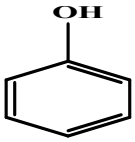	100	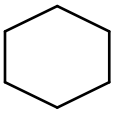	36
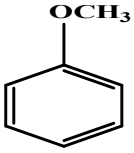	81	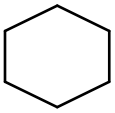	29
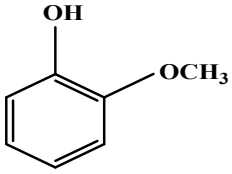	54	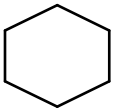	20
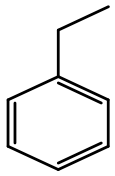	98	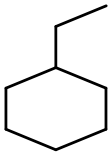	36
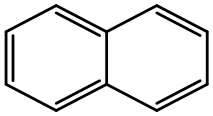	40	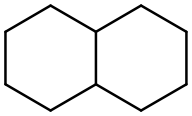	15
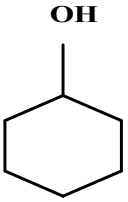	100	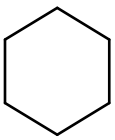	36

Reaction conditions: *m*-Cresol :2 mmol, T=170 °C, P=2 MPa, t = 6 h, Solvent: *n*-Dodecane (2 mL); Catalyst = 8 mol. % of Ni (0.05 g).

References

1 R.V. Jasra, J. Das, A. Unnikrishnan and A. Sakthivel, 2016, US Patent 9359216B2

2 Spectral Database for Organic Compounds, https://sdbs.db.aist.go.jp/sdbs/cgibin/cre_index.cgi (accessed October 30)